

# H $\alpha$ MORPHOLOGIES AND ENVIRONMENTAL EFFECTS IN VIRGO CLUSTER SPIRAL GALAXIES

REBECCA A. KOOPMANN

Union College and  
 Department of Physics, Schenectady, NY 12308

JEFFREY D. P. KENNEY

Astronomy Department and  
 Yale University, P.O. Box 208101, New Haven, CT 06520-8101

(Received 2002 August 23)

Accepted 2004 June 3

## ABSTRACT

We describe the various H $\alpha$  morphologies of Virgo Cluster and isolated spiral galaxies, and associate the H $\alpha$  morphologies with the types of environmental interactions which have altered the cluster galaxies. The spatial distributions of H $\alpha$  and R-band emission are used to divide the star formation morphologies of the 52 Virgo Cluster spirals into several categories: normal (37%), anemic (6%), enhanced (6%), and (spatially) truncated (52%). Truncated galaxies are further subdivided based on their inner star formation rates into truncated/normal (37%), truncated/compact (6%), truncated/anemic (8%), and truncated/enhanced (2%). The fraction of anemic galaxies is relatively small (6-13%) in both environments, suggesting that starvation is not a major factor in the reduced star formation rates of Virgo spirals. The majority of Virgo spiral galaxies have their H $\alpha$  disks truncated (52%), whereas truncated H $\alpha$  disks are rarer in isolated galaxies (12%). Most of the H $\alpha$ -truncated galaxies have relatively undisturbed stellar disks and normal-to-slightly enhanced inner disk star formation rates, suggesting that ICM-ISM stripping is the main mechanism causing the reduced star formation rates of Virgo spirals. Several of the truncated galaxies are peculiar, with enhanced central star formation rates, disturbed stellar disks, and bar-like distributions of luminous HII complexes inside the central 1 kpc, but no star formation beyond, suggesting recent tidal interactions or minor mergers have also influenced their morphology. Two highly-inclined H $\alpha$ -truncated spirals have numerous extraplanar HII regions, and are likely in an active phase of ICM-ISM stripping. Several spirals have one-sided H $\alpha$  enhancements at the outer edge of their truncated H $\alpha$  disks, suggesting modest and local enhancements in their star formation rates due to ICM-ISM interactions. Low-velocity tidal interactions and perhaps outer cluster HI accretion seem to be the triggers for enhanced global star formation in four Virgo galaxies. These results indicate that most Virgo spiral galaxies experience ICM-ISM stripping, many experience significant tidal effects, and many experience both.

*Subject headings:* galaxies: spiral — galaxies: clusters: general — galaxies: clusters: individual (Virgo) — galaxies: fundamental parameters — galaxies: peculiar — galaxies: structure

## 1. INTRODUCTION

Many kinds of environmental interactions have been proposed to affect galaxies in clusters, yet it is still unknown which processes actually occur and the key details of what happens in the different kinds of interactions.

Processes which tend to affect the gas content of the galaxy, but not the existing stellar content, include (i) intracluster medium - interstellar medium (ICM-ISM) interactions (Gunn & Gott 1972; Nulsen 1982; Schulz & Struck 2001; Vollmer et al. 2001; van Gorkom 2004) which selectively remove ISM gas from galaxies and might also compress the ISM and trigger star formation, (ii) gas accretion, which would presumably occur in the cluster outskirts, and (iii) starvation or strangulation, the stripping of gas from a galaxy's surroundings which might otherwise have accreted onto the galaxy (Larson, Tinsley, & Caldwell 1980; Balogh, Navarro, & Morris et al. 2000). Tidal or gravitational effects (Toomre & Toomre 1972; reviews by Struck 1999 and Mihos 2004), which affect both stars and gas, are also likely to be im-

portant, and include (i) low-velocity tidal interactions and mergers, which can occur both inside and outside of clusters, (ii) high-velocity tidal interactions and collisions, which occur almost exclusively in clusters (e.g., Moore, Lake, & Katz 1998), and (iii) tidal interactions between galaxies and the cluster as a whole, or sub-units within clusters (Byrd & Valtonen 1990).

There have been a number of recent studies of environmental processes in nearby and distant cluster galaxies with authors reaching a variety of conclusions (see review by O'Connell 1999) concerning star formation histories and lenticular formation. They can be roughly divided into four categories: (i) those which suggest that the major influence on spirals in clusters is ICM-ISM stripping, which reduces star formation mainly by simple truncation, although modest bursts may happen in at least some galaxies (e.g., Abraham et al. 1996; Bravo-Alfaro et al. 2000, 2001; Jones, Smail, & Couch 2000; Couch et al. 1998). (ii) those which suggest that starbursts caused by tidal interactions with the cluster or other galaxies have had a major effect on the evolution of a significant number of galaxies (e.g., Moss & Whittle 2000; Caldwell et al.

1996; Caldwell, Rose, & Dendy 1999; Henrikson & Byrd 1996; van Dokkum et al. 1999; Rose et al. 2001). (iii) those which suggest that the reduction in cluster galaxy star formation has been gradual (Balogh et al. 1999) or occurs also in the outer cluster (Treu et al. 2003), more consistent with starvation than (complete) ICM-ISM stripping. (iv) those which suggest that at least 2 of the above processes, e.g., ICM-ISM stripping and tidal interactions are necessary to explain observed star formation properties (Poggianti et al. 1999; 2001). It is interesting that different studies disagree about the main environmental effects even when analyzing the same cluster! Taken together, the results of these studies indicate that the properties of cluster galaxies may be determined by a variety of environmental interactions over a Hubble time (e.g., Miller 1988; Oemler 1992; Moore et al. 1998) and may vary between clusters, and over time. On the other hand, the complexity and disagreement shows that detailed studies of star formation in cluster galaxies are needed.

In this paper we try to establish a link between the  $H\alpha$  morphologies of Virgo Cluster spirals and the types of interaction(s) which may have affected them. The spatial distribution of  $H\alpha$  emission is a sensitive indicator of some types of environmental interactions, since it traces part of the ISM, as well as star formation activity. We have chosen to study galaxies in the Virgo Cluster, the nearest moderately rich cluster, so that we can study cluster interactions at the highest possible resolution.

This paper is one of a series based on our  $H\alpha$  and R imaging survey of Virgo Cluster and isolated spirals galaxies. We present the observational data for the Virgo galaxies in Koopmann et al. (2001, hereafter PI) and that for the isolated galaxies in Koopmann & Kenney (2004, in prep, hereafter PII). These papers include  $H\alpha$  and R images and radial profiles for all galaxies. In a companion paper (Koopmann & Kenney 2004, hereafter PIII), we present a detailed comparison of  $H\alpha$  radial distributions and star formation rates of the Virgo and isolated galaxies, finding that truncation of the star-forming disk is the main reason for reduced Virgo star formation rates, but that the star formation rates of individual Virgo spirals range from reduced to enhanced. In this paper, we describe more fully the different types of  $H\alpha$  radial distributions and morphologies, and use this and other information in an attempt to determine the types of environmental effects which have altered the Virgo spirals.

## 2. STAR FORMATION MORPHOLOGIES IN THE VIRGO CLUSTER

In Papers I, II, and III, we present R and  $H\alpha$  images, radial profiles, integrated fluxes, and concentration indices for 55 Virgo Cluster and 29 isolated S0-spiral galaxies which are brighter than  $M_B = -18$ , and have inclinations less than  $75^\circ$ . In this paper we exclude the S0's, and consider a sample of 52 Virgo Cluster and 24 isolated Sa-Scd galaxies. In Paper III, galaxies were compared via the Hubble types, as well as the several quantitative measures of the radial distributions and relative amounts of R and  $H\alpha$ , which we also use in this paper. The central R light concentration,  $C30$ , is the inverse ratio of R-band flux within the 24 magnitudes per arcsec $^{-2}$  isophote,  $r_{24}$ , and the  $0.3 r_{24}$  isophote. This is a measure of the stellar

TABLE 1  
MEDIAN ISOLATED SPIRAL  $H\alpha$  EQUIVALENT WIDTHS

Radial Bin	EW (Å)	EW (Å)
	$0.20 \leq C30 \leq 0.40$	$0.41 \leq C30 \leq 0.60$
$0 < r < 0.1r_{24}$	21	6
$0.1r_{24} < r < 0.3r_{24}$	19	10
$0.3r_{24} < r < 0.5r_{24}$	32	19
$0.5r_{24} < r < 0.7r_{24}$	34	15
$0.7r_{24} < r < 1.0r_{24}$	30	13
Total	35	15

light central concentration, and a tracer of the bulge-to-disk ratio.  $CH\alpha$  is an analogous quantity for the  $H\alpha$  concentration, i.e. the ratio of  $H\alpha$  flux within  $0.3r_{24}$  to that within  $r_{24}$ . The normalized massive star formation rate (NMSFR) is the ratio of  $H\alpha$  flux to R flux, measured within the same aperture, and is similar to an equivalent width.

In Paper III, we show that truncation of the star forming disk is the most common cause of reduction in star formation in the Virgo Cluster by examining radial profiles and integrated NMSFRs. In this paper, we wish to quantify the numbers of galaxies affected by truncation, as well as other types of star formation reduction or enhancement, using objective, comparative measures of a galaxy's  $H\alpha$  and R radial profile. We base our definitions on the values of NMSFR for the 5 radial bins ( $r < 0.1r_{24}$ ,  $0.1r_{24} < r < 0.3r_{24}$ ,  $0.3r_{24} < r < 0.5r_{24}$ ,  $0.5r_{24} < r < 0.7r_{24}$ , and  $0.7r_{24} < r < 1.0r_{24}$ ) shown in Figure 8 of Paper III. In order to define a 'normal' NMSFR for isolated galaxies, we binned the isolated sample spiral galaxies (Sa-Scd) into low concentration ( $C30 \leq 0.40$ ) and high concentration ( $C30 > 0.40$ ) classes. Each bin contained 12 galaxies. We computed the low and high concentration median isolated NMSFR for each of the radial bins and compared these values to the NMSFRs of individual galaxies of high and low concentrations in each radial bin. We then looked for trends of enhancement or reduction over multiple bins of the star-forming disk of each galaxy in order to define several star formation morphology classes. A second iteration was made removing the four isolated galaxies which fit into categories other than 'normal'. Table 1 presents the isolated median rates (in units of equivalent width) derived for each bin.

We define the following star formation morphology classes:

(N) **Normal:** spirals with global NMSFRs within a factor of 3 of the isolated global medians, as well as NMSFRs within a factor of 5 of the isolated median in the innermost ( $r < 0.1r_{24}$ ) bin, and NMSFRs within a factor of 3 in at least three of the other four radial bins. In most cases, these galaxies are within a factor of 3 of the isolated median for each radial bin. However, enhancements/reductions of a factor greater than 3 do occur within single bins for several galaxies, due to the 'bumpiness' of the  $H\alpha$  distribution, which can be caused by barred regions, rings of star formation, and circumnuclear activity. In two cases (1 isolated, 1 Virgo) the innermost (circumnuclear) bin rate is enhanced or reduced

by 3-5 times. We have elected to include these galaxies in the normal category because the circumnuclear bin contains the center of the galaxy and is therefore most susceptible to color-dependent continuum subtraction errors and contamination by the [NII] line. In a few cases (6 isolated, 1 Virgo), one of the other four bins is enhanced or reduced by slightly more than a factor of 3. Examination of the H $\alpha$  image shows that these reductions/enhancements are due either to bars or rings of star formation.

(A) **Anemic:** spirals which have low but measurable NMSFR across all radial bins. The requirements to fit into this class are a global NMSFR reduced by at least a factor of 3 together with a detectable NMSFR in all bins which is reduced by at least a factor of 2. The detectability of the NMSFR was confirmed by inspection of the radial H $\alpha$  profile and the H $\alpha$  images.

(E) **Enhanced:** spirals with global NMSFRs enhanced by at least a factor of three compared to isolated medians.

(T) **Truncated:** spirals with a sharp cutoff in the star-forming disk, with a reduction in NMSFR of at least 10 times in the outermost (0.7 - 1.0 $r_{24}$ ) bin. This requirement selects galaxies with truncation radii smaller than about 0.8  $r_{24}$ .

About half (52%) of the Virgo Cluster spirals have truncated star-forming disks. We subdivide these galaxies based on their inner disk star formation rates and morphologies into the following classes:

(T/N) **Truncated/Normal:** spirals with ‘normal’ inner disk NMSFRs interior to the truncation radius, where ‘normal’ is defined as above. Interior to the truncation radius, the H $\alpha$  surface brightness distribution is similar to that of the large scale disk in the R band. (This is in contrast to the Truncated/Compact galaxies, described in the next class.)

Within this class, one can further distinguish between those with severe truncation (truncation radius less than 0.4 $r_{24}$ ), or moderate truncation (truncation radius between 0.4-0.8 $r_{24}$ ). Galaxies with mild truncation (truncation radius greater than 0.8 $r_{24}$ ) also exist, but these are hard to unambiguously identify with our data, so in this paper are in the Normal class.

(T/C) **Truncated/Compact:** spirals with circumnuclear ( $r < 0.1r_{24}$  bin) NMSFRs enhanced by at least a factor of 5, together with a reduction of at least a factor of 10 in the outermost 2 bins. In these galaxies, the H $\alpha$  radial surface brightness profile is much steeper than that of the large scale disk at every radius, and closer to that of a “bulge”, with much of the emission concentrated in the central 1 kpc. This class of H $\alpha$  morphology is distinct from a Truncated/Normal galaxy with a severe truncation, which has an H $\alpha$  radial profile similar to that of the large scale disk inward of the truncation radius. In Truncated/Compact galaxies, most of the H $\alpha$  emission arises from a non-axisymmetric distribution of luminous circumnuclear HII complexes.

(T/A) **Truncated/Anemic:** spirals with detectable NMSFRs in the innermost bins which are reduced in level by at least a factor of 2 compared to the innermost isolated bin medians.

(T/E) **Truncated/Enhanced:** spirals with NMSFRs enhanced by at least a factor of 3 above isolated medians in at least two bins interior to the truncation radius.

TABLE 2  
POPULATIONS OF STAR FORMATION CLASSES FOR CLUSTER AND ISOLATED ENVIRONMENTS

Star Formation Class	Isolated	Virgo
Normal	83% (20)	37% (19)
Enhanced	0%	6% (3)
Anemic	4% (1)	6% (3)
Truncated/Normal	8% (2)	37% (19)
Truncated/Compact	4% (1)	6% (3)
Truncated/Anemic	0%	8% (4)
Truncated/Enhanced	0%	2% (1)
Truncated (all)	12% (3)	52% (27)
Anemic (all)	4% (1)	13% (7)
Enhanced (all)	0%	8% (4)

NOTE. — Percentages and numbers of isolated and Virgo Cluster galaxies in the star formation classes described in Section 2. The last three rows sum the total numbers of truncated galaxies and the total numbers of galaxies with anemia or enhancement over at least part of the star-forming disk.

Table 2 gives the percentages of Virgo and isolated spirals in each class and Table 3 the class assignment of Virgo galaxies.

The definition of these classes involves the computation of NMSFRs over 5 radial bins in a galaxy. A second method of discriminating between the different H $\alpha$  morphologies, which is simpler although less accurate, is based on a plot of the total NMSFR versus the H $\alpha$  concentration parameter, CH $\alpha$ . Figure 1 shows that these two parameters discriminate fairly well between the classes. The good separation of classes in the plot suggests that this type of approach may be useful in identifying trends in star formation morphologies in large samples of galaxies. Starburst galaxies would also be well-separated in the plot. As shown in the figure, central starbursts would have an elevated global NMSFR and a high H $\alpha$  concentration, since most of the enhanced star formation is occurring in the center. Global starbursts would have a lower H $\alpha$  concentration, because of enhanced star formation throughout the disk. However, this approach does not work perfectly for all galaxies. For example, it does not distinguish between truncated/compact galaxies and truncated/normal galaxies with severe truncation, since for these galaxies the H $\alpha$  radial profile differs inside the radius of 0.3 $r_{24}$  which is used in the definition of CH $\alpha$ .

The median profiles of the classes are compared in Figure 2. (See PIII for an explanation of how median H $\alpha$  profiles are derived.) Shading indicates the interquartile range. The first panel provides a comparison between isolated low- $C30$  and high- $C30$  spirals, which are similar within the interquartile range over most of the disk. In the remaining panels, the Virgo normal median and range is compared to the isolated low- $C30$  and the other classes of Virgo spirals. The normal Virgo spiral median is significantly different from the other classes, except the low- $C30$  isolated spirals (although there is a clear tendency toward mild truncation at radii beyond  $r_{24}$  for the Virgo normal spirals).

There is little correlation with star formation class and  $C30$ , as shown in Figure 3. The galaxies in each class show a range in  $C30$ . Anemic galaxies show the least range, with all three Virgo anemic galaxies and the iso-

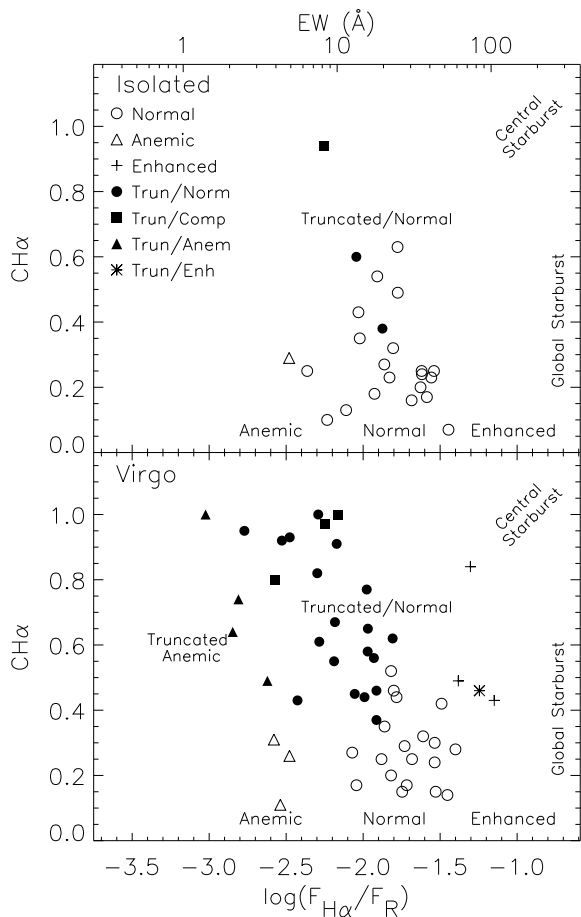


FIG. 1.—  $H\alpha$  concentration vs the global NMSFR for the Virgo sample. The symbols indicate the  $H\alpha$  morphology class, which is defined by the radial distribution of star formation (Section 2). The upper x-axis provides the equivalent width scale. The  $H\alpha$  morphology classes can be well-discriminated using these two parameters.

olated anemic galaxy at higher  $C30$  of 0.42 - 0.52 (see also Bothun & Sullivan 1980). Two of four truncated/anemic galaxies also have higher  $C30$  values of about 0.5, but the other two have low  $C30$ 's of 0.33-0.4.

The star formation classes are further discussed in sections 2.1- 2.4, giving specific galaxy examples. In Sections 2.5 and 2.6, we discuss two other interesting subsets of galaxies: galaxies with star formation enhanced locally near the truncation radius and several apparent pairs in the Virgo Cluster. In Section 2.7, the locations of galaxies of each class within the cluster are compared. Section 2.8 provides a comparison of  $H\alpha$  and HI morphologies.

### 2.1. Virgo Spirals with Normal Star Formation Rates Within $r_{24}$

About one-third (37% ; 19 galaxies) of the Virgo Cluster sample spirals have star formation rates similar to those of isolated spirals within  $r_{24}$ . These galaxies span the full range of  $C30$  and are classified later-type spirals (3 Sb and 16 Sc). Apparently these galaxies have not experienced a strong and/or recent environmental interaction. These galaxies may be recent arrivals in the cluster. Although these galaxies do not show significant dif-

ferences in star formation rates from the isolated spirals, some appear to have mildly truncated  $H\alpha$  profiles, while others display other peculiarities. For example, NGC 4654 has a peculiar  $H\alpha$  distribution and an HI tail and may be experiencing an ICM-ISM encounter (Phookun & Mundy 1995), perhaps in addition to a galaxy-galaxy tidal encounter (Vollmer 2003). NGC 4651 appears as a relatively normal Sc within  $r_{24}$ , but deep optical images reveal a peculiar linear feature and several shell-like features at large radii (Schneider & Corbelli 1993; Malin 1994), which may be caused by a minor merger. Some of these galaxies also show asymmetric outer arcs of star formation, possibly indicating ICM pressure (Section 2.5).

### 2.2. Anemic Virgo Spirals

Anemic galaxies were first defined based on the arm-interarm contrast in the disk (van den Bergh 1976), which is related both to gas content (Elmegreen et al. 2002) and star formation activity. Historically, the term ‘anemia’ has sometimes been used to refer to any galaxy with a reduced global star formation rate. The spatial resolution of our study allows us to define anemia more specifically as a low but measurable  $H\alpha$  surface brightness *across the disk*. Neither the arm-interarm contrast nor the global star formation rate distinguish between truncation and anemia. Three Virgo Cluster galaxies and one isolated galaxy (IC 356) fall in the anemic class. Images and radial profiles of the Virgo cluster galaxies are shown in Figure 4. Four additional Virgo spirals are anemic galaxies which also have truncated star-forming disks (see Section 2.3.3). The few anemic galaxies tend to fall in the lower left-hand corner of Figure 1, with low global star formation rates and normal to low  $H\alpha$  concentration.

The dividing line between normal and anemic star formation is somewhat arbitrary. For example, if we chose to define anemic galaxies as galaxies which have NMSFRs reduced by at least three times in all radial bins, the number of anemics in the Virgo Cluster falls from 3 to 1 and in the isolated sample from 1 to 0. The paucity of anemic galaxies shows that global anemia does not play a dominant role in reduction of total star formation rates among the Virgo spirals. While the star formation of some Virgo galaxies may indeed appear weak across the disk, isolated galaxies can have equally weak disk star formation (as also pointed out for a sample of nearby galaxies by Bothun & Sullivan 1980).

Anemic galaxies should not be confused with low surface brightness galaxies. Anemic galaxies have low  $H\alpha$  surface brightness with respect to the continuum, while low surface brightness galaxies have low continuum and low-to-intermediate  $H\alpha$  surface brightnesses. Because we normalize the  $H\alpha$  emission by the R continuum brightness, the NMSFRs of low surface brightness galaxies fall in regions of our plots similar those of high surface brightness galaxies.

It is illustrative of the past approach of anemic classification to compare the classifications of van den Bergh (1976) and van den Bergh, Pierce, & Tully (1990). They classify NGC 4548 as anemic, but NGC 4394 as a normal spiral. They list a number of other galaxies in our sample as anemic, including (i) NGC 4424, 4457, 4522, 4569, and 4580, which we find to be severely truncated, (ii) NGC 4579, and 4689, which are less severely truncated, (iii)

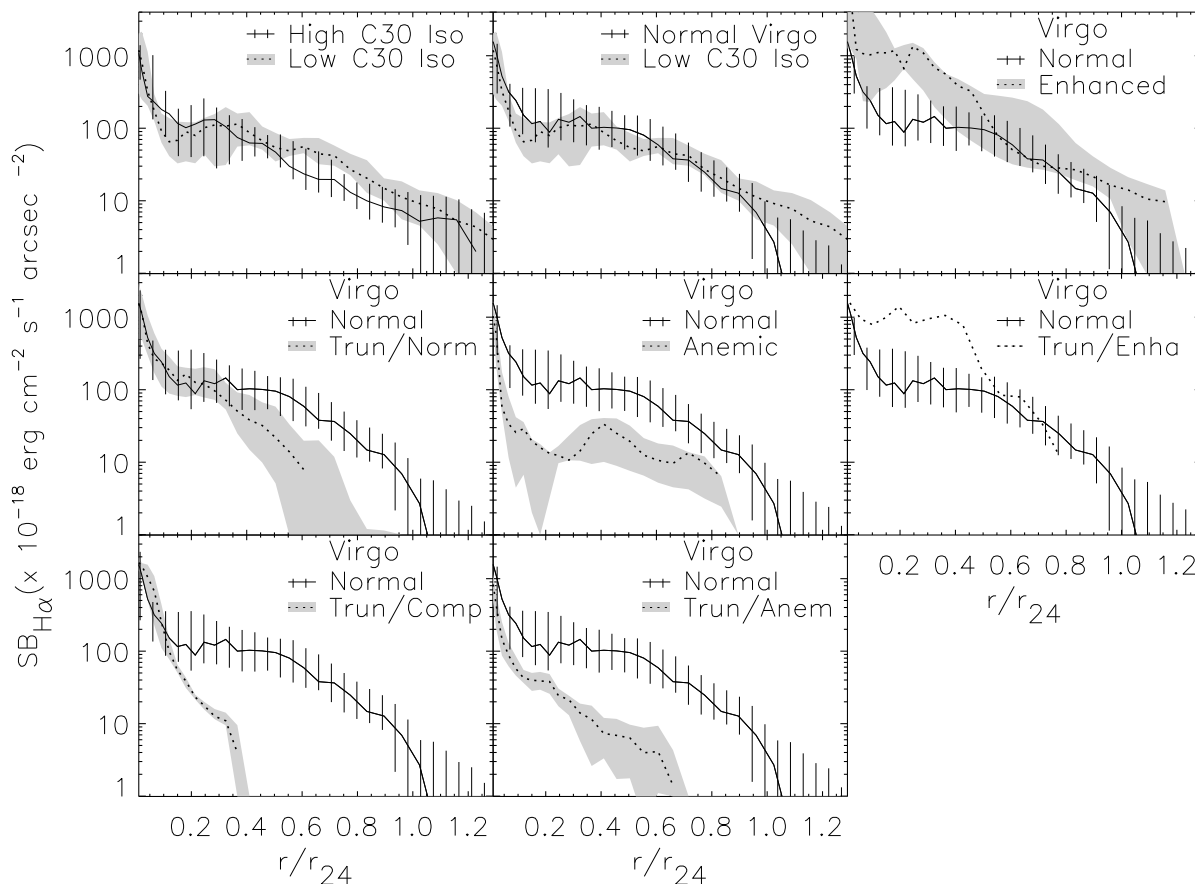


FIG. 2.— Median H $\alpha$  radial profiles and plotted with interquartile range for various classes of galaxies. In the first panel, the low ( $C30 < 0.4$ ) and high concentration ( $C30 > 0.4$ ) isolated galaxies are plotted with the indicated shading. The radial distribution of star formation in isolated galaxies of the two concentration ranges is similar over much of the star forming disk. In the second panel, the low  $C30$  isolated galaxy median is also similar to the normal Virgo star formation morphology class. In the remaining panels, galaxies in the normal Virgo spiral class are significantly different from the median of other star formation morphologies over much of the disk.

NGC 4293 and NGC 4450 which are truncated/anemic (iv) NGC 4651, which is normal, and (v) NGC 4643, 4710, and 4429, which do not have detectable HII regions. We reemphasize that the term anemic, as used in the past, has been applied to a variety of star formation distributions.

### 2.3. Virgo Spirals with Truncated Star-Forming Disks

Just over half (52% ; 27 galaxies) of the Virgo sample show truncation in the star-forming disk within  $0.8r_{24}$ . This class of star-formation morphology is therefore by far the most common in the Virgo Cluster. The severity of truncation varies, from moderate truncation in the outer half of the disk (from  $0.4-0.8 r_{24}$ ) (16), to severe truncation at radii less than  $0.4 r_{24}$  (11). The star formation morphology within the truncation radius also varies, from normal (19) to enhanced (1) to anemic (4) to compact (3).

The severely truncated galaxies were referred to as ‘St’ by Koopmann & Kenney (1998). In this paper, we give these galaxies a more detailed designation according to their star formation morphology, which is either truncated/normal or truncated/compact.

#### 2.3.1. Truncated Spirals with Normal Inner Disks

The largest subclass of truncated galaxies are those which have normal or slightly enhanced inner star formation rates compared to isolated spirals. Eight galaxies are severely truncated, with normal-to-slightly enhanced (up to a factor of 3.3) star formation within  $0.3-0.4r_{24}$ , but no star formation in the disk outside this radius.

Three galaxies, NGC 4580, NGC 4405, and IC 3392, have severely truncated H $\alpha$  disks with enhanced star formation at the H $\alpha$  truncation radius, but appear fairly normal inside the truncation radius. These galaxies were assigned ‘mixed’ Hubble-type classifications of Sc/Sa and Sc/S0 by Binggeli, Sandage, & Tammann (1985; hereafter BST) because of their peculiar morphology. The R images (Figure 5) show that the stellar disks beyond the edge of the star-forming disk are mostly regular and featureless, except for NGC 4580, which has spiral arms. NGC 4580 and IC 3392 have symmetric rings of star formation near the truncation radius, containing a large fraction of the H $\alpha$  emission. NGC 4405 has a knottier and asymmetric HII region distribution, with an arc or partial ring to the southwest. H $\alpha$  major axis spectra of all three galaxies show regular, rising rotation curves for the ionized gas (Rubin, Waterman, & Kenney 1999). The truncated H $\alpha$  distribution, combined with the regular stellar isophotes and regular gas kinematics, strongly

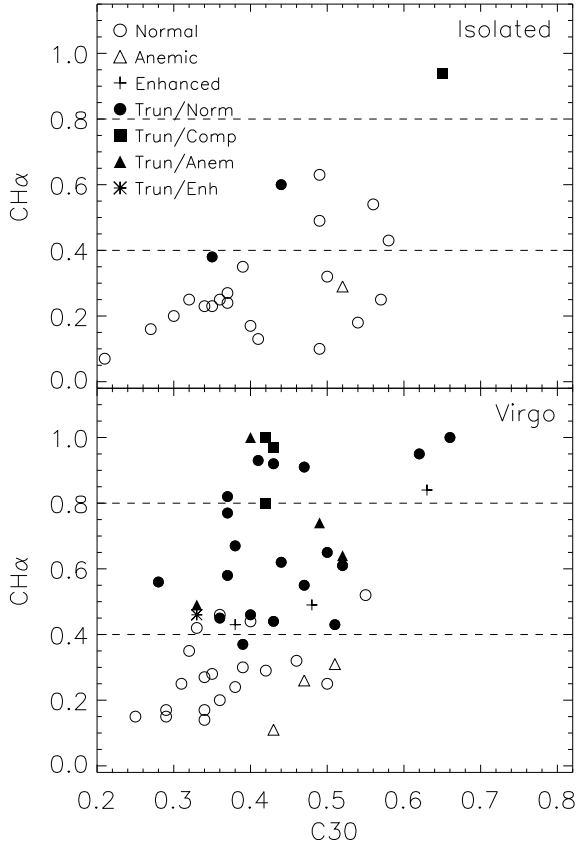


FIG. 3.— Comparison of  $C30$  and  $CH\alpha$  for the different star formation classes, showing little correlation between  $C30$  and the star formation morphology.

suggest that these galaxies are victims of ICM-ISM stripping.

Two severely truncated galaxies with apparently extraplanar HII regions (NGC 4522 and NGC 4569) are shown in Figure 6. While the stellar disk of the highly inclined NGC 4522 appears relatively undisturbed, the  $H\alpha$  and HI emission show a truncated disk and extraplanar gas reminiscent of a bow shock morphology (Kenney & Koopmann 1999; Kenney, van Gorkom, & Vollmer 2004). This strongly suggests that the ISM of NGC 4522 is being stripped by the gas pressure of the ICM. NGC 4569 has smooth, relatively featureless, outer spiral arms and a ring of star formation at  $0.3 r_{24}$ . A distinct peculiar arm of HII regions, which begins at the  $H\alpha$  truncation radius and has an HI counterpart (Vollmer et al. 2004), may be extraplanar (Hensler et al. 2003). This arm resembles the one-arm gas morphologies commonly seen in the ICM-ISM interaction simulations of Schulz & Struck (2001) and Vollmer et al. (2001).

NGC 4351, also shown in Figure 6, has a strongly asymmetric, off-center, patchy distribution, with a high surface brightness in the circumnuclear region. The HI emission is highly asymmetric in the same direction as the  $H\alpha$  emission (Warmels 1988). NGC 4351 is one of the galaxies closest to the cluster center, only  $1.7^\circ$  from M87, and it has a high line-of-sight velocity of  $2310 \text{ km s}^{-1}$ . The location of the galaxy and the combination of more regular R isophotes and asymmetric  $H\alpha$  and HI emis-

sion make this galaxy a good candidate for an ongoing ICM-ISM interaction.

The severely truncated galaxy NGC 4457 (image given in PI) has a regular R morphology and a nearly circular outer ring, which suggests we are viewing the galaxy close to face-on. The galaxy has a relatively strong but truncated  $H\alpha$  disk with much of the  $H\alpha$  emission arising from one peculiar spiral arm. While this arm may resemble those seen in ICM-ISM simulations (Schulz & Struck 2001), NGC 4457 is located  $9^\circ$  from M87 where the ICM is thought to be very tenuous.

Of the eight galaxies in the truncated/normal (severe) category, the amorphous galaxy NGC 4694 seems least consistent with ICM-ISM stripping. Its  $H\alpha$  profile is borderline truncated/anemic galaxy or truncated/compact. NGC 4694 features a complex dust morphology (Malkan, Gorjian, & Tam 1998), low major axis velocities, (Rubin et al. 1999), and a peculiar HI distribution, with a small central concentration of HI and a 40 kpc HI tail extending to the neighboring dwarf irregular galaxy VCC 2062 (van Driel & van Woerden 1989; see also Hoffman et al. 1996). van Driel & van Woerden (1989) conclude that an interaction with an intergalactic gas cloud is most likely the explanation for the structure of NGC 4694, although an interaction with VCC 2062 or another galaxy is possible.

The remaining eleven  $H\alpha$  truncated galaxies have less severely truncated star-forming disks, with truncation radii of  $0.4\text{--}0.8 r_{24}$ . They also have more HI than galaxies with severely truncated  $H\alpha$  disks, with HI deficiency parameters ranging from 0.07–0.81 (HI deficient up to a factor of 7). Two isolated galaxies, NGC 613 and IC 5273, also have moderately truncated  $H\alpha$  profiles.

### 2.3.2. Virgo Spirals with Compact Star-Formation

Three Virgo Cluster spirals have extremely small  $H\alpha$  disks, with HII complexes distributed asymmetrically and only within the central kpc. All have  $M_B$  between  $-18$  and  $-19$ , and all are strongly HI deficient.

These include two Virgo galaxies with the most unusual  $H\alpha$  morphologies of our sample: NGC 4424 and NGC 4064, which have compact  $H\alpha$  emission from several circumnuclear HII complexes, as shown in Figure 7. The  $H\alpha$  surface brightnesses of these two galaxies within  $0.1 r_{24} \sim 0.8 \text{ kpc}$  are among the highest in the Virgo and isolated samples (see also Figure 2), and most of the  $H\alpha$  emission originates in HII complexes with luminosities of  $L_{H\alpha} = 5 \times 10^{38} \text{ erg s}^{-1}$ .  $H\alpha$  major axis spectra show low line-of-sight velocities inconsistent with circular motions in the plane suggested by the outer optical isophotes (Rubin et al. 1999). NGC 4424 has unusual heart-shaped inner R isophotes and shell-like features (Kenney et al. 1996) similar to those seen in simulations of mergers (e.g., Hernquist & Quinn 1988; Hernquist 1992, 1993), suggesting that NGC 4424 is the product of a recent minor merging event (Kenney et al. 1996). NGC 4064 has a more regular R morphology than NGC 4424. It shows very open spiral arms and a bar in the center. The peculiar dust morphology also suggests a recent minor merger or tidal interaction (Cortés & Kenney, in prep.). Strongly HI-deficient with no gas detected in their outer disks, these galaxies probably have experienced ICM-ISM stripping in addition to mergers.

The other truncated/compact galaxy NGC 4606 has

FIG. 4.— Three Virgo Cluster galaxies with anemic star formation, i.e., reduced star formation rates across the disk. In this and the following figures, the R and H $\alpha$  images and surface photometry profiles are given for each galaxy. The images are displayed on a log scale, with north up and east to the left. The RSA/BST and RC3 morphological types are indicated. In the surface photometry plots, the R (solid) and H $\alpha$  (dotted) profiles are plotted as a function of radius in arc seconds. The H $\alpha$  profiles were superposed using an arbitrary zeropoint of 18.945. The H $\alpha$  profile is cut at the radius of the outermost HII region. At upper right the galaxy positions are shown on top of a ROSAT x-ray map of the Virgo cluster (Böhringer et al. 1994). At lower right, large filled circles identify the galaxies in the C30-NMSFR plot (see PIII, Figure 8). In the following figures, additional galaxies within a class are indicated by smaller fonts in the cluster map and smaller filled circles in the C30-NMSFR plot. Note how the indicated anemic galaxies fall at low star formation rates globally, in the inner 30% of the disk, and in the outer 70% of the disk.

FIG. 5.— Three Virgo Cluster galaxies with severely truncated star-forming disks (within  $0.4r_{24}$ ). These galaxies have regular stellar disks and their H $\alpha$  morphologies show symmetric rings of star formation near the truncation radius. These galaxies have likely been stripped by the ICM. The galaxies are indicated in the cluster map by large font lettering and in the C30-NMSFR plot by large filled circles. The locations of other galaxies with severely truncated H $\alpha$  disks are indicated in the cluster map with smaller font and in the C30-NMSFR plot with small filled circles. See Figure 4 for details on the plots.

fainter H $\alpha$  emission, consisting of  $\sim 3$  faint HII complexes, distributed in a linear feature extending from the center toward the southwest and almost coincident with the major axis. A possible companion is NGC 4607 (separation of  $4' = 18$  kpc and  $593 \text{ km s}^{-1}$ ).

The *isolated* severely truncated galaxy, NGC 4984, has a compact star-forming disk with active star formation distributed in an incomplete nuclear ring. The galaxy has a high C30 and is classified as Sa and a starburst (Devereux 1989; Kewley et al. 2001). Thus severely truncated H $\alpha$  disks do occur in isolated galaxies, perhaps also triggered by minor mergers or tidal interactions with low surface brightness companions.

### 2.3.3. Truncated Spirals with Anemic Inner Disks

Four galaxies have truncated star-forming disks with anemic star formation within the truncation radius. All are classified as Sa by BST and/or by deVaucouleurs (1991; hereafter RC3), although two (NGC 4293 and NGC 4380) have C30 values similar to isolated Sb or Sc galaxies. Images of three of them are shown in Figure 8.

NGC 4380, NGC 4419, and NGC 4450 appear to have regular stellar morphologies. NGC 4380 has weak star formation over much of the disk within the truncation radius of  $0.7r_{24}$ , and a sharp ridge of H $\alpha$  emission on the northwest side suggestive of ICM pressure. The highly inclined NGC 4419 has a strongly asymmetric CO distribution (Kenney et al. 1990), suggesting an ongoing ICM-ISM interaction. In contrast, NGC 4293 has a disturbed stellar morphology suggesting a tidal disturbance or minor merger.

Three additional galaxies, NGC 4579, NGC 4694 and NGC 4772, can be considered borderline truncated/anemic. All have NMSFRs which are low across the disk, but by slightly less than a factor of two, and so are classified as truncated/normal. The Southern Extension galaxy NGC 4772 shows kinematic signatures of a past minor merger (Haynes et al. 2000), and NGC 4694 exhibits peculiarities suggestive of a tidal interaction (Section 2.3.1).

### 2.3.4. Truncated Spirals with Enhanced Total Star Formation Rates

The only sample galaxy with both enhanced star formation and a truncated H $\alpha$  disk is NGC 4299. Its global H $\alpha$  equivalent width of  $84\text{\AA}$  is one of the 3 highest values in the Virgo sample, and its H $\alpha$  image (Figure 9) shows numerous bright HII regions throughout a disk truncated

beyond  $0.7r_{24}$ . The outer extent of the H $\alpha$  distribution is irregular, except in the southwest where it forms a well-defined ridge extending over  $90^\circ$ , suggesting ongoing ICM pressure. The most luminous HII complex in the galaxy is located at the southern end of this ridge. NGC 4299 is in an apparent pair with NGC 4294, which is projected  $5.8'$  (27 kpc) away, and has a similar line-of-sight velocity. NGC 4294 is similar to NGC 4299 in mass, luminosity, morphology, HI content, and a relatively high global star formation rate. Unlike NGC 4299, there is no clear ridge of HII regions at the outer edge of the H $\alpha$  disk. The high rates of star formation in these galaxies might be due a tidal interaction, perhaps enhanced in NGC 4299 due to an ongoing ICM-ISM interaction. The location of this pair, only  $2.4^\circ$  from M87, makes an ICM-ISM interaction plausible.

### 2.4. Virgo galaxies with enhanced inner and total star formation rates

Six percent (3 galaxies) of the Virgo sample has total and inner star formation rates much higher than those in the isolated sample, and one additional galaxy (discussed separately in Section 2.3.4) has an enhanced inner disk combined with a truncated outer disk. Three of these enhanced galaxies are intermediate mass galaxies with  $M_B$  between -19 and -18, and one is massive, with  $M_B = -21$ .

The 3 Virgo sample galaxies with the highest normalized massive star formation rates are NGC 4383, NGC 4532, and the Truncated/Enhanced galaxy NGC 4299. (Figure 9) The normalized star formation rates of spiral galaxies are a function of both luminosity and morphological type (Boselli et al. 2001), and these 3 galaxies have total NMSFRs which are 2.5-5 times higher than the isolated median, and 2-3 times larger than any isolated sample galaxy of similar luminosity or central concentration (PIII). Compared to the isolated galaxies, the inner NMSFRs of these galaxies are even more extreme than the total NMSFRs, with values 3-4 times larger than any isolated sample galaxy (see Figures 4 and 8 of Paper III). The total H $\alpha$  equivalent widths of these 3 galaxies are  $70\text{--}100\text{\AA}$ , which is somewhat higher than those in the nearby, well-known starburst galaxies M82 and NGC 1569 (Kennicutt & Kent 1983). All have equivalent widths which are on the high end of the distribution shown by Boselli et al. (2001) for galaxies in many environments, for the appropriate galaxy luminosity. Nearly all non-cluster spiral galaxies with H $\alpha$

FIG. 6.— Three Virgo Cluster galaxies with star forming disks truncated within  $0.4r_{24}$ , normal-enhanced inner star formation rates, and peculiar  $H\alpha$  distributions, possibly extraplanar emission. NGC 4569 has a ring of star formation at about  $0.3r_{24}$  and a detached arm of HII regions, which may be extraplanar (Hensler et al. 2003). NGC 4522 appears to interacting with the ICM, based on the extraplanar HII regions and disturbed HI and radio continuum (Kenney & Koopmann 1999; Kenney et al. 2004). The  $H\alpha$  emission in NGC 4351 is offset from the apparent center in R. See Figure 4 for details on the plots.

FIG. 7.— Three Truncated/Compact Virgo spirals. These galaxies have severely truncated star-forming disks. Star formation is located in several circumnuclear HII complexes, which have a non-axisymmetric distribution. The  $H\alpha$  surface brightnesses of NGC 4424 and NGC 4064 within  $0.1r_{24} \sim 0.8$  kpc are among the highest in the Virgo and isolated samples. The gas in these galaxies has low line-of-sight velocities (Rubin et al. 1999). NGC 4424 also displays shell-like features and banana-shaped isophotes (Kenney et al. 1996). These galaxies are likely to be products of a merger or close tidal interaction. See Figure 4 for details on the plots.

equivalent widths above  $60\text{\AA}$  are strongly disturbed or in galaxy pairs (Kennicutt et al. 1987).

The Sm/Im galaxy NGC 4532 has the highest NMSFR in the Virgo sample, with an  $H\alpha$  equivalent width of  $88\text{\AA}$ . Its  $H\alpha$  image (Figure 9) shows vigorous star formation throughout the galaxy, with no sharp outer boundary in  $H\alpha$  that would indicate ICM pressure. The galaxy is moderately HI-rich (HI def = -0.35), and both NGC 4532 and the nearby DDO137 are associated with a large extended, bi-lobal, HI cloud (Hoffman et al. 1993). Much of the HI is concentrated around the 2 optical galaxies, but about one-third seems kinematically and spatially distinct from the individual galaxies (Hoffman et al. 1999). The enhanced star formation in NGC 4532 might therefore be caused by tidal forces and/or gas accretion.

NGC 4383 is an amorphous (BST) galaxy with a large bulge-to-disk ratio ( $C30=0.63$ ). Most of the isolated galaxies of similar concentration are S0 galaxies without significant HII regions. The  $H\alpha$  image shows a biconical filamentary structure strongly suggestive of a starburst outflow, numerous HII regions in the central 2 kpc, and an irregular string of bright HII regions extending into the outer galaxy. The dS0 galaxy UGC 7504 (VCC 794), 3.3 magnitudes fainter than NGC 4383, is very nearby in projection ( $2.5' = 12$  kpc), with a line-of-sight velocity difference of  $800 \text{ km s}^{-1}$ , and no  $H\alpha$  emission. NGC 4383 is HI rich (HI def = -0.53) and has no sharp outer boundary in  $H\alpha$ , suggesting that a process other than ICM pressure, probably a tidal interaction and/or gas accretion, is responsible for its enhanced star formation.

The third enhanced Virgo galaxy, NGC 4303, is one of the largest spirals in Virgo ( $M_B = -21$ ). It has an  $H\alpha$  equivalent width of  $61\text{\AA}$ , which is unusually high for a large mass spiral (Boselli et al. 2001).

The Virgo galaxies with the highest NMSFRs are all HI normal to HI rich, and preferentially  $H\alpha$ -enhanced in the inner galaxy. All have apparent nearby companions, which suggests that low-velocity tidal interactions may play a role in the enhancement in star formation rates, as in observed in galaxy pairs outside of clusters (Kennicutt et al. 1987). At least one of them is associated with a large, extended cloud of HI, suggesting that HI accretion, perhaps combined with tidal forces, plays a role in the enhanced star formation rates.

There is evidence that ICM-ISM interactions enhance the NMSFR of some Virgo galaxies, but with the possible exception of NGC 4299 (Section 2.3.4), the enhancements appear to be local and globally modest. As discussed in Section 2.5, there are a number of other Virgo galaxies whose  $H\alpha$  morphologies are strongly suggestive

of locally enhanced NMSFR due to ICM pressure.

## 2.5. Galaxies with Enhanced Outer Disks?

One might expect an additional class of galaxies with significantly enhanced outer disks. Such a morphology might arise from ICM induced star formation in a galaxy. However, only 3 Virgo Cluster galaxies (NGC 4519, NGC 4713, NGC 4532), show evidence for outer disk star formation rates which are enhanced above levels seen in isolated galaxies, and these galaxies also have high NMSFRs in their inner disks. As discussed in Section 2.4, the star formation properties of these galaxies are most likely influenced by tidal interactions or gas accretion.

Seven spirals show asymmetric enhancements in star formation at the outer edge of the  $H\alpha$  disk. These enhancements are modest, since in none of the galaxies do the NMSFRs measured in any radial bin exceed the values found for isolated spirals (see Figure 8 in Paper III). The  $H\alpha$  distributions in these galaxies range from severely truncated (NGC 4405, Figure 5), to normal (NGC 4178, NGC 4189, and NGC 4654, Figure 10), and 1 is truncated/anemic (NGC 4380, Figure 8). Two are in apparent close pairs (NGC 4298 and NGC 4647, Figure 11), and a third may also be in a binary pair (NGC 4654, Vollmer 2003), and in these cases the roles of tidal and ICM effects are unclear. For the 4 systems not in pairs, the  $H\alpha$  morphologies are just what is expected from ongoing ICM pressure. These asymmetric enhancements are different from the axisymmetrically enhanced outer  $H\alpha$  rings in the  $H\alpha$ -truncated galaxies NGC 4580 and IC 3392 (Section 2.3.1). Guided by the simulations of Schulz & Struck (2001) and Vollmer et al. (2001), we suggest that those galaxies with asymmetrically enhanced outer  $H\alpha$  edges are presently experiencing ICM pressure, whereas those with symmetric outer rings may be observed after peak pressure, when the truncated gas disks ‘anneals’ (Schulz & Struck 2001).

## 2.6. Pairs in the Virgo Cluster

At the high relative velocities characteristic of many tidal encounters in clusters, the interacting partners move away from each other so quickly that the occurrence of a tidal interaction, the participants, and the interaction parameters are hard to determine. One category of tidal interaction where the interacting galaxies can be identified is bound pairs.

We have analyzed the magnitudes, velocities, and positions of galaxies in the Virgo Cluster Catalog (BST) to assess the significance of apparent pairs in the cluster. We have identified apparent pairs which include at least one galaxy brighter than  $B=14$  ( $M_B = -17$ ), are similar in mass with a blue magnitude difference of less than 3,

FIG. 8.— Three Truncated/Anemic Virgo Cluster galaxies. These galaxies have truncated star-forming disks and anemic inner star formation rates. NGC 4380 and NGC 4293 are classified as Sa galaxies, but both have a small central R light concentration. The sharp ridge of H $\alpha$  emission to the northwest in NGC 4380 is suggestive of ICM interaction. The stellar morphology of NGC 4293 is disturbed, possibly due to a tidal interaction. See Figure 4 for details on the plots.

FIG. 9.— Three Virgo Cluster galaxies with enhanced or truncated/enhanced star formation. There is evidence for tidal forces and/or gas accretion in all three cases. The truncated/enhanced galaxy NGC 4299 may plausibly be experiencing an ICM-ISM interaction. In the C30-NMSFR plot, NGC 4299 is indicated by a filled square. Note the relatively high position of all of the enhanced galaxies in the C30-NMSFR diagram and that these galaxies tend to be located in the cluster outskirts. All of these galaxies except NGC 4303 have  $M_B$  between -18 and -19. See Figure 4 for details on the plots.

and are close together on the sky, with a position difference of less than  $10'$  ( $= 45$  kpc projected). There are 61 such pairs in Virgo, and 49 of these have measured velocities for both galaxies, according to BST. The probability that the apparent pairs are due to chance superpositions along the line-of-sight can be estimated by assuming a Maxwellian distribution of velocity differences (e.g., Binney & Tremaine 1987). For a cluster velocity dispersion of  $\sigma=700$  km s $^{-1}$ , one would expect only 2 pairs with velocity differences less than 200 km s $^{-1}$ , whereas 16 such low-velocity pairs exist. This clear excess implies that most of these low-velocity apparent pairs are true pairs.

Four of these low velocity pairs are in our Virgo sample, and three are shown in Figure 11. All of these galaxies have at least mildly truncated H $\alpha$  disks. Two have asymmetric H $\alpha$  enhancements at the truncation radius, on the side closest to the companion, as well as asymmetric R morphologies (NGC 4298 and NGC 4647). Two others, NGC 4294/4299 (Figure 9) have mildly to strongly enhanced H $\alpha$  equivalent widths, similar to the enhancements observed in some non-cluster pairs (Kennicutt et al. 1987).

Since tidal interactions affect both stars and gas, it is likely that ICM-ISM interactions and not tidal interactions are responsible for the truncated gas disks + asymmetric stellar morphologies in these Virgo pair galaxies. This is consistent with the location of these pairs, all of which are projected within  $3.2^\circ$  from M87. Thus, these galaxies have likely experienced both ICM-ISM and tidal interactions. The presence of these pairs, but the absence of recent major mergers in the Virgo Cluster suggests that the most of the pairs may be disrupted by tidal interactions with other galaxies or the cluster before they can merge.

### 2.7. Location of Galaxies by Class in the Cluster

The locations of the different H $\alpha$  classes on a ROSAT x-ray map of the Virgo cluster (Böhringer et al. 1994) are shown in the upper right panels of Figures 4- 11 and Figure 12. Figure 13 shows the radial distribution in the cluster of each H $\alpha$  type. For this plot, we have divided the Virgo sample into 3 radial bins:  $\leq 3^\circ$ ,  $3^\circ$ - $4.5^\circ$ , and  $\geq 4.5^\circ$ , with about one-third the total sample in each.

Inside  $3^\circ$ ,  $\sim 80\%$  of the galaxies are truncated in some way, and only  $\sim 10\%$  of the galaxies are normal. In the inner  $2^\circ$ , all 7 of the sample galaxies are truncated. The fraction of galaxies which are truncated in some way decreases strongly with radius, to 50% in the mid-cluster, and 30% in the outer cluster (see also Dale et al. 2001).

Normal H $\alpha$  types also vary strongly with radius. There are no normal galaxies within  $2.4^\circ$  of M87, but beyond  $3^\circ$  about half of the galaxies are H $\alpha$ -normal. Several of

the ‘H $\alpha$ -normal’ galaxies in the intermediate radial bin actually seem to be H $\alpha$ -truncated very far out in their disks.

The anemic, enhanced, truncated/compact, and truncated/anemic radial distributions are all roughly flat, within the errors, although there are no more than 2 galaxies in any radial bin. The outer cluster ( $\geq 4.5^\circ$ ) contains half the anemic and enhanced galaxies, but only 15% of the truncated/normal galaxies.

While truncated galaxies are clearly concentrated toward the center, some are found far out. Some could have been stripped in the past and carried on highly radial orbits into the outer cluster. Mamon et al (2004) find that the maximum radius reached by a galaxy which has passed through the inner cluster to be 1-2.5 virial radii, which in Virgo is about 1.7-4.1 Mpc. The outer cluster truncated/normal galaxies are well within this limit. Some outer cluster truncated galaxies appear more peculiar than simply ISM-stripped spirals (e.g., NGC 4694, NGC 4772; see Section 2.3.1), and their ISM properties may not be due to stripping in a core passage (see also Sanchis, Lokas, & Mamon 2004).

The lower right panel of Figure 12 shows the positions of the nine candidates for systems presently experiencing ICM pressure, including extraplanar HII regions (Section 2.3.1) or asymmetrically enhanced outer H $\alpha$  arcs (Section 10). While, this sample of galaxies is not chosen as objectively as our H $\alpha$  classes, it does give some indication of where ICM pressure may be affecting the galaxies. The figure shows evidence for active ICM pressure out as far as about  $4.5^\circ$  from M87, or 1 Abell radius, which is beyond the x-ray contours shown in Figure 12. ROSAT has detected x-ray emission further out than is shown in Figure 12, although it is hard to know its precise extent due to confusion with galactic emission (Böhringer et al. 1994).

These results suggest that anemia and starbursts are caused by mechanisms which operate throughout the cluster, even in the outskirts, such as galaxy-galaxy tidal interactions. Truncation is caused by a mechanism which operates most effectively in the cluster center, such as ICM-ISM stripping.

### 2.8. H $\alpha$ and HI Morphologies of Sample Galaxies

In Paper III we find a strong correlation between the H $\alpha$ -based NMSFR and the HI deficiency parameter. In this section, we compare the H $\alpha$  morphologies with HI radial morphologies. Cayatte et al. (1994) describe 4 types of HI profiles for 17 Virgo Cluster spirals: Group I galaxies have normal HI distribution over most of disk compared to field spirals, Group II galaxies have lower inner HI densities and somewhat truncated outer distri-

FIG. 10.— Three Virgo Cluster galaxies which show locally enhanced  $H\alpha$  emission in asymmetric arcs near the edge of the star-forming disk. NGC 4380 (Figure 8) and pair galaxies NGC 4298 and NGC 4647 (Figure 11) also show similar outer arcs of star formation. However this local enhancement is not significant enough to increase the NMSFR over the whole radial bin, as shown at lower left. (See Figure 4 for details on the plot, but note that, unlike preceding figures, the plot at lower right depicts the NMSFRs within three smaller radial bins:  $0.3r_{24} < r < 0.5r_{24}$ ,  $0.5r_{24} < r < 0.7r_{24}$ , and  $0.7r_{24} < r < 1.0r_{24}$ .)

FIG. 11.— Three apparent pairs in the Virgo Cluster. These galaxies appear close in projection and have similar line-of-sight velocities. Another apparent pair is NGC 4294/4299 (see Figure 9). Note that a few galaxies are enhanced globally (NGC 4294 and NGC 4299) and all have substantial inner star formation. See Figure 4 for details on the plots.

FIG. 12.— Cluster locations of galaxies of the indicated  $H\alpha$  classes on a ROSAT x-ray map of the Virgo cluster (Böhringer et al. 1994). The x-ray peak coincides with the giant elliptical M87, and secondary peaks correspond to M86 ( $1.5^\circ$  W of M87), and M49 ( $4.5^\circ$  W of M87), each of which are associated with sub-clusters. Similar maps for other classes are found in the upper right panel of Figures 4–11. No normal galaxies are found within  $2.4^\circ$  of M87, while truncated/normal galaxies are typically found closer to the cluster center. Anemic galaxies are found throughout the cluster. Galaxies which have extraplanar HII regions or asymmetric  $H\alpha$  enhancements at the outer edge of a truncated  $H\alpha$  disk (shown in plot at lower right) are located up to  $4.5^\circ$  from M87. Such galaxies may be presently experiencing ICM pressure.

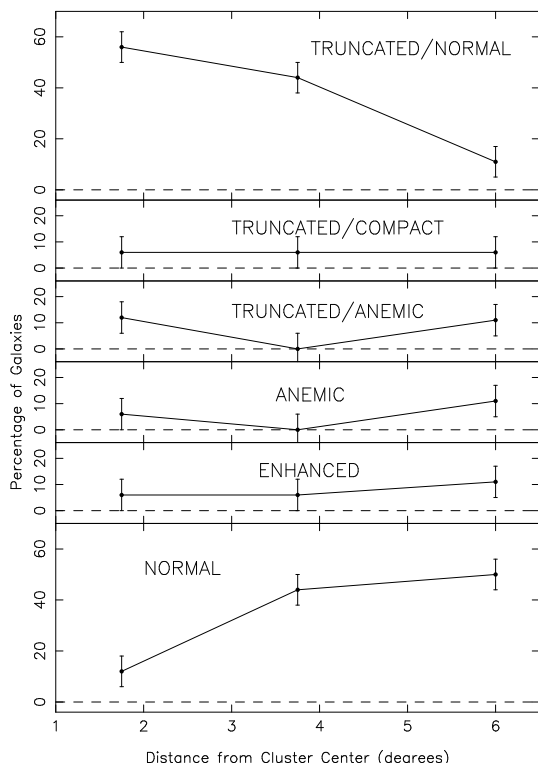


FIG. 13.— Cluster radial distributions of each  $H\alpha$  class, plotted as percentages of all the galaxies in that radial bin. Bins are  $\leq 3^\circ$ ,  $3^\circ$ – $4.5^\circ$ , and  $\geq 4.5^\circ$ . Error bars correspond to 1 galaxy, comparable to the uncertainty in our  $H\alpha$  classification. There is a clear radial dependence for the normal and truncated/normal classes, with fewer normal and more truncated/normal galaxies closer to the cluster center. Other  $H\alpha$  classes have a flatter distribution (but contain fewer sample galaxies).

butions, Group III galaxies have severely truncated HI distributions, but similar central surface density to field spirals, and Group IV galaxies have a low surface density of HI as well as a central HI hole. We have eleven galaxies in common with the sample of Cayatte et al. Figure 14 shows the HI group designation of these galaxies in the

$C30 - F(H\alpha)/F(R)$  plot. There is a clear correlation, although not a perfect one-to-one correspondence, between the HI and  $H\alpha$  radial distributions. The galaxies with severely truncated HI disks (III) also have the most truncated  $H\alpha$  disks. The most anemic galaxies in  $H\alpha$  are generally those with low HI surface densities across the disk (IV). Galaxies with more peculiar HI morphologies also tend to have peculiar  $H\alpha$  morphologies.

Figure 15 compares HI and  $H\alpha$  radii, normalized by optical radii, for the Virgo sample. The HI radii are derived from HI maps by Warmels (1988), Cayatte et al. (1994), Kenney et al. (2004) and Crowl (2004, in prep.). The  $H\alpha$  radius is defined as the radius containing 95% of the  $H\alpha$  emission ( $r_{H\alpha 95}$  in PI). There is a good correlation between the HI and  $H\alpha$  radii, with HI radii typically 0–100% larger than  $H\alpha$  radii. Galaxies with  $H\alpha$ -truncated disks also have HI-truncated disks, although the HI radii are somewhat larger on average. This may be partly because star formation is inhibited or very inefficient in the outermost gas of truncated spirals, just as it is in regular spirals, due, for example, to an insufficient threshold density for star formation (Kennicutt 1989). But it is also partly due to low resolution (typically  $30$ – $45''$ ) for most of the HI measurements, which can result in an overestimate of the true HI diameter. For those few truncated galaxies with higher ( $\sim 15''$ ) resolution HI observations, the radii ratios are closer to 1.

The good overall agreement between HI and  $H\alpha$  distributions indicates that  $H\alpha$  is a reasonable tracer of the environmental effects on the ISM. In particular, the  $H\alpha$ -truncated galaxies all have truncated HI distributions, with HI diameters similar to or slightly larger than their  $H\alpha$  diameters. This can be understood as a natural outcome of the requirement of a threshold density for star formation (Kennicutt 1989). It also indicates that  $H\alpha$  truncation is due to a truncated gas disk, rather than a gas disk which is simply not forming stars, due to an increased threshold density for star formation.

### 3. ENVIRONMENTAL EFFECTS IN THE VIRGO CLUSTER

In the preceding sections, we began to link the  $H\alpha$  morphologies of cluster galaxies with the environmental effects experienced by them. In this section we further establish the links, and discuss the implications of our results for cluster galaxy evolution.

#### 3.1. ICM-ISM Interactions

The truncation of the star-forming disks in the majority of Virgo Cluster spirals, particularly those with regular stellar isophotes, is strong evidence that ICM-ISM interactions are significant in the evolution of Virgo Cluster galaxies. The strong central concentration in

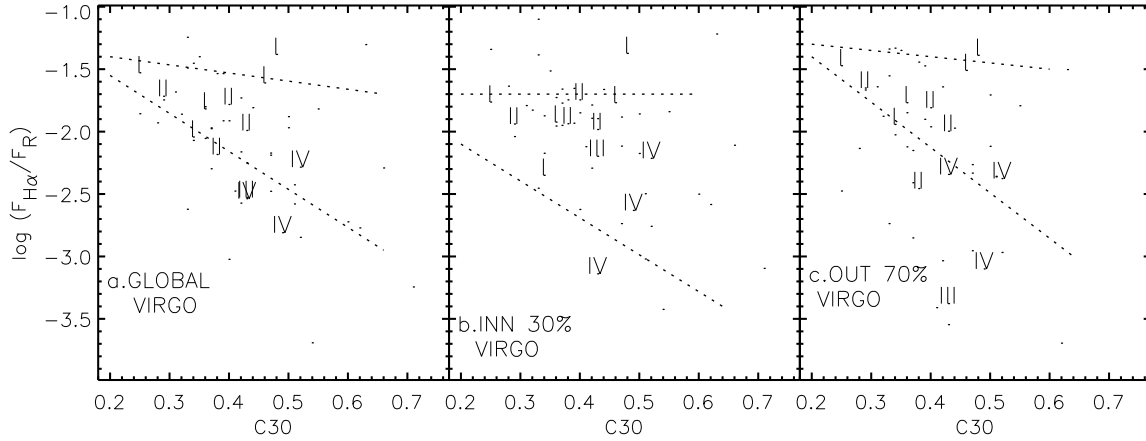


FIG. 14.— NMSFRs versus central concentration parameter  $C30$  for (a) the whole galaxy, (b) the inner 30% of the optical disk, and (c) the outer 70% of the optical disk, for the Virgo sample. The Roman numerals indicate the HI morphologies described by Cayatte et al. (1994). There is a clear trend between HI radial morphology and star formation rates.

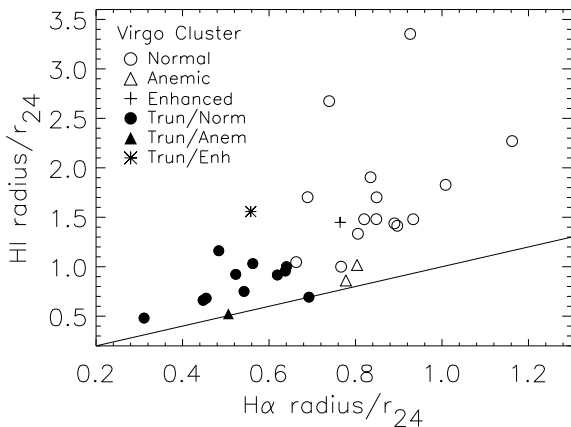


FIG. 15.— Comparison of H $\alpha$  radii to HI radii for galaxies with HI maps (Warmels 1988; Cayatte et al. 1994; Kenney et al. 2004; Crowl 2004, in prep.). The symbols indicate the H $\alpha$  morphology classes. There is a good correlation between H $\alpha$  and HI radii. In particular, galaxies with truncated H $\alpha$  disks also have truncated HI disks.

the cluster of truncated galaxies supports the association of truncation with ISM stripping by the ICM. The normal to slightly-enhanced star formation rates in the inner galaxy disks imply that ICM-ISM interactions have not had a large effect on the inner regions of most Virgo spiral galaxies. Modest local H $\alpha$  enhancements in some of the Virgo sample galaxies are strongly suggestive of ICM pressure (Section 2.5), but those Virgo galaxies with the largest global and inner star formation rate enhancements appear to be more strongly affected by processes other than ICM pressure. While large enhancements in star formation may be caused by ICM-ISM interactions in some clusters (e.g., Dressler & Gunn 1983; Gavazzi et al. 2001), in Virgo the enhancements due to ICM pressure seem to be modest and local.

Truncated gas disks in galaxies with relatively undisturbed stellar disks are predicted from simple physical considerations of ICM-ISM interactions (Gunn & Gott 1972), and are seen in 3D simulations (Abadi, Moore, & Bower 1999; Quilis, Moore, & Bower 2000; Schulz &

Struck 2001; Vollmer et al 2001). The key parameters of an ICM-ISM interaction are the ICM pressure, which in turn depends on the ICM density and the velocity of the galaxy with respect to the ICM, and the disk angle with respect to the ICM wind direction. All of these vary as a galaxy follows its orbital path within the cluster, and the present state of a galaxy depends on this orbital history. Of particular importance is the time since (until) maximum ram pressure. Since many HI-deficient galaxies in clusters have highly radial orbits (Dressler 1986; Solanes et al. 2001), the ram pressure can vary by factors of 20-100 during the orbit, and gas may even fall back into the galaxy after being pushed outward (Vollmer et al. 2001). The interaction also depends on the properties of the galaxy and its ISM, particularly the total mass distribution and the ISM mass distribution. In addition, what we observe depends on the viewing angle between the vector of the galaxy's motion through the ICM and the line-of-sight. The oldest galaxies in the cluster have made 5-10 orbits, although each orbit will be different in the changing potential of the accreting, growing, lumpy, unrelaxed cluster. A challenge is to recognize the effects of these various parameters in particular galaxies, and to identify the evolutionary stages of the interactions.

Some progress has been made distinguishing active from past stripping. Simulations indicate that truncated gas disks can survive for much more than  $10^8$  yr (Schulz & Struck 2001), so some of the Virgo spirals with truncated gas disks were likely stripped a long time ago. However, galaxies with extraplanar HII regions or asymmetric H $\alpha$  enhancements at the outer edges of truncated gas disks are likely experiencing active ICM pressure (Section 2.5). Among the best examples of active ICM-ISM stripping in the Virgo Cluster is NGC 4522, a highly inclined spiral with a normal stellar disk, truncated HI, H $\alpha$  and radio continuum disks, and extraplanar emission from all 3 ISM tracers displaced to one side of the disk (Kenney & Koopmann 1999; Kenney et al. 2004). The opposite, leading edge of the galaxy has enhanced polarized radio emission, and the flattest spectral index, suggesting ongoing ICM pressure (Vollmer et al. 2004). Apart from the extraplanar HII regions, the truncated H $\alpha$  morphology of NGC 4522 resembles the majority of

Virgo spirals.

The combination of a galaxy's rotation with its forward motion relative to the ICM create an asymmetric ram pressure (Kritsuk 1983). Simulations including the effects of rotation on ICM-ISM interactions show in some phases one dominant extraplanar gas arm emerging from the outer edges of truncated gas disk (Vollmer et al. 2001; Schulz & Struck 2001). Such arms may be observed in NGC 4548 (Vollmer et al. 2000), NGC 4654 (Phookun & Mundy 1995; Vollmer 2003), and NGC 4569 (Vollmer et al. 2004; Hensler et al. 2003; Kenney et al. in prep). Simulations show that the arms can transfer angular momentum from the inner gas disk, which can make a contracted, denser, 'annealed' inner gas disk, which has some resistance to further stripping (Schulz & Struck 2001). A couple of the Virgo galaxies (NGC 4580, IC 3392; see Figure 5) show rings of enhanced star formation at the truncation radius, which resemble the annealed gas rings of Schulz & Struck (2001).

### 3.2. Galaxy-Galaxy Interactions

Gravitational interactions between galaxies vary from mergers and accretions to penetrating collisions to non-penetrating encounters. The variety in collision parameters, particularly mass ratio, impact parameter, and relative velocity, results in a range of effects on the colliding galaxies. Non-merging tidal encounters are common in clusters, and multiple, fast tidal encounters may strongly influence a galaxy's morphology over a Hubble time (Miller 1988; Moore et al. 1998). Simulations of merging galaxies of similar mass show that extensive tidal tails containing stars and gas are produced (e.g., Toomre & Toomre 1972; see also Hibbard 1995). Deep imaging of Virgo Cluster galaxies shows some galaxies with low surface brightness tails (Malin 1993), which have likely been caused by gravitational interactions. Since tails in clusters are quickly destroyed by cluster tidal fields (Mihos 2004), the Virgo galaxies with observed tails are a small fraction of the cluster merger and collision populations. A likely example of a recent, high-velocity tidal encounter is the disturbed Virgo Cluster galaxy NGC 4438, which may have experienced a direct collision (Kenney et al. 1995; Kenney & Yale 2002). The H $\alpha$  emission is dominated by a peculiar one-sided filamentary H $\alpha$  nebula associated with the interaction, although the global star formation rate is modest.

There is evidence for major and intermediate-mass ratio mergers in many Virgo galaxies, including the ellipticals M87, M49, and NGC 4365 (Gavazzi et al. 2000; Lee, Kim, & Geisler 1997; Davies et al. 2001), the S0's NGC 4550, NGC 4382, NGC 4262, NGC 4643 (Rubin, Graham, & Kenney 1992; Rix et al 1992; Schweizer & Seitzer 1988; van Driel and van Woerden 1991; Richter, Sackett, & Sparke 1994), and the Sa's NGC 4698 and NGC 4772 (Bertola et al. 1999; Haynes et al. 2000). Most of these mergers probably occurred  $>1$  Gyr ago, since the galaxies do not appear very disturbed. There are no obvious candidates for an ongoing major merger in the Virgo Cluster; however, there is at least one clear case in the Coma Cluster (Bravo-Alfaro et al. 2001) and merger galaxies are frequently seen in higher- $z$  clusters (van Dokkum et al. 1999). There are clear examples of recent minor mergers, even among the Sc galaxies. The Virgo spiral NGC 4651, which appears as a relatively

normal Sc within  $r_{24}$ , has a peculiar linear feature and several low surface brightness shell-like features at large radii (Schneider & Corbelli 1993; Malin 1994), suggesting a recent minor merger. Its star formation rate and distribution are not that peculiar, and its H $\alpha$  class is normal. Thus H $\alpha$  is not an especially good tracer of old mergers or recent minor mergers although we note that NGC 4698 is anemic and NGC 4772 is borderline truncated/anemic, so anemia may result from some types of mergers.

In our Virgo survey, H $\alpha$  distributions classified as enhanced or truncated/compact are likely caused by tidal interactions, including minor mergers. The H $\alpha$  morphologies of the 3 Virgo galaxies with the largest star formation rates, NGC 4299, NGC 4383, and NGC 4532 seem consistent with those seen in non-cluster tidally interacting systems. In these systems, enhancements are observed in both the global and nuclear NMSFRs, but the enhancements are generally greater near the center (Kennicutt 1998). The inward gas flow and strongly enhanced circumnuclear star formation in the truncated/compact galaxies NGC 4424 (Kenney et al. 1996) and NGC 4064 (Cortés & Kenney, in prep.) are likely due to recent minor mergers. Tidal interactions are expected to occur throughout the cluster, including the outskirts, where lumpy infall is occurring. This is consistent with the locations of galaxies with enhanced and truncated/compact H $\alpha$  profiles, which are found throughout the cluster.

These H $\alpha$ -selected tidally interacting galaxies are only a fraction of all tidally interacting galaxies. Rubin et al. (1999) find disturbed kinematics in  $\sim 50\%$  of Virgo galaxies, suggesting that tidal encounters are frequent in the Virgo Cluster (see also Dale et al. 2001). Although tidal interactions can clearly cause enhancements in the star formation rate, there is not a one-to-one correspondence between the strength of the tidal interactions and the star formation rate. In the majority of tidal interactions, star formation enhancements are modest (Kennicutt 1998). This is consistent with the moderately enhanced star formation rates observed in some of the Virgo galaxies in apparent pairs (Section 2.6). Thus H $\alpha$  may not be a good tracer of all dynamical effects caused by collisions and tidal interactions. Some of this is timescale: the enhanced star-forming phase, if any, may be short-lived, compared to the time that the galaxy is dynamically disturbed, and experiencing significant radial mass transfer and dynamical heating of the disk.

### 3.3. Gravitational and ICM-ISM Stripping?

Many Virgo galaxies should be affected by multiple types of interactions, since a large fraction of spirals show evidence of stripping (this paper), and most Virgo spirals have either disturbed rotation curves (Rubin et al. 1999) or show some other evidence for tidal interactions.

While tidal interactions are clearly an important process driving cluster galaxy evolution, it is doubtful that tidal interactions alone could be responsible for most spiral-S0 transformations. The combination of tidal interactions with ICM-ISM stripping can drive the evolution of spirals toward a lenticular state. Strong tidal interactions typically drive inner gas inward and outer gas outward in tidal tails, depleting the gas at intermediate radii (e.g., Barnes & Hernquist 1991). Some of the gas

driven toward the center forms stars, yielding a galaxy with a higher central concentration of stars, although not necessarily a bulge. However, most tidal interactions will not clean out the outer disk of star-forming gas, and this is probably required for a galaxy to be classified as lenticular. ICM-ISM stripping seems to be required for the disk cleaning, although tidal interactions can make a galaxy more susceptible to ICM-ISM stripping by driving some of the outer disk gas outward, where it becomes easier to strip. In this way a tidal interaction can facilitate the stripping of the ISM by the ICM. This combination of effects is likely for the truncated/compact H $\alpha$  class of galaxies including NGC 4064 and NGC 4424. These spiral galaxies should become small bulge S0 galaxies within 1 Gyr.

### 3.4. Starvation

Larson, Tinsley, & Caldwell (1980) proposed a ‘starvation’ model, in which the normal gaseous inflow which fuels ongoing star formation in spirals is cut off in clusters, as spirals fall into the cluster for the first time. Abraham et al. (1996) and Balogh et al. (1999, 2000) find that the evolution of the galaxies in several clusters is consistent with a significant reduction in star formation rather than starbursts. A reduction could be caused by either ICM-ISM stripping or starvation. Starvation would be gradual whereas ICM-ISM stripping would be relatively abrupt, but may not be complete since a central gas disk can survive. Based on the relatively small number of k+a galaxies, with strong Balmer absorption lines but no emission lines, Balogh et al. (1999, 2000) suggest that the reduction in star formation is not abrupt and complete, but is instead more gradual. This would occur with starvation (also called ‘strangulation’ by Balogh & Morris 2000), but might also be consistent with abrupt partial ICM-ISM stripping. Treu et al. (2003) find evidence for a possible difference in the morphological mix of galaxies between the field and the region outside the virial radius ( $r \sim 1-2$  Mpc from the cluster center) of the in the  $z=0.4$  cluster Cl0024+16, and suggest that starvation and tidal effects may be significant processes in the outer cluster.

The simulations of Bekki et al. (2002) show that starvation leads to gas and star formation distributions which closely resemble anemic spirals, with lowered rates of star formation throughout the disk. Gas infall, or its curtailment, should not have a radial dependence strong enough to produce sharply truncated gas disks. If the primary mechanism for gas loss were starvation, we might therefore expect to see a large fraction of anemic spirals, particularly since starvation occurs on a much longer timescale than disk gas stripping.

The fraction of purely anemic galaxies in the 2 environments is similar (6% Virgo, 4% isolated). 8% of the Virgo sample, but none of the isolated sample, are classified as truncated/anemic. The origin of the H $\alpha$  distributions in these 4 systems may be diverse (Section 2.3.3). Some appear tidally disturbed, whereas others could be anemic disks that were truncated, or spirals that were truncated a long time ago and have now faded into anemia. Even if all the purely anemic and truncated/anemic galaxies in Virgo are added together, the total anemic fraction is 14% in Virgo and 4% isolated. The fraction of anemic galaxies is somewhat higher in Virgo, although low in

both environments. If starvation causes anemia, these results indicate that starvation is not the main cause of reduced star formation in the Virgo cluster.

### 3.5. Summary

The spatial distributions of star formation in Virgo Cluster and isolated spirals provide evidence that both ICM-ISM stripping and tidal interactions have had a major influence on the evolution of Virgo Cluster spiral galaxies.

H $\alpha$  is a good tracer of active gas stripping and past partial gas stripping. Gas stripping can significantly and irreversibly diminish the future star formation potential of a galaxy, and the truncated star forming disk in partially stripped galaxies will likely remain apparent for more than  $10^9$  years. Among the truncated/normal spiral galaxies, the most severe truncation is  $0.3r_{24}$ . If a galaxy is stripped much more severely, it may be classified as an S0. NGC 4710 is an edge-on Virgo S0 with abundant molecular gas and star formation in the central 2 kpc =  $0.2r_{24}$  (Wrobel & Kenney 1992), and is a good candidate for an S0 created by severe but incomplete ICM-ISM stripping. Fully stripped spirals become S0s, although it is not possible to tell from its H $\alpha$  properties whether a galaxy became an S0 via complete stripping or some other process. Since the most severely stripped spirals become S0’s, which are not in our sample, ICM-ISM stripping likely affects an even larger fraction of spirals than indicated by our study.

H $\alpha$  should also be a good tracer of starvation. The future star formation potential of a galaxy is greatly and probably irreversibly diminished by arrested gas infall, and the anemic star forming disk will likely remain apparent for more than  $10^9$  years. Thus the large number of H $\alpha$ -truncated galaxies compared to H $\alpha$ -anemic galaxies should be a reflection of the greater importance of ICM-ISM stripping than starvation for cluster galaxy evolution.

H $\alpha$  is certainly sensitive to some tidal effects, but probably less sensitive to tidal effects than to gas stripping or starvation. Many galaxies that experience tidal encounters experience enhanced star formation, but only for brief intervals. Other tidally interacting galaxies do not have greatly altered star formation rates (Kennicutt 1998), yet they probably experience radial gas inflow and disk heating from the tidal encounters. For all but mergers and the strongest tidal encounters, the long term star formation potential may not be greatly altered, and in many cases, it will be hard to tell  $10^9$  years later that the galaxy had a tidal interaction from the H $\alpha$  properties. Thus in contrast to gas stripping or starvation, we only see those galaxies which are presently experiencing tidal encounters in H $\alpha$ . Overall, tidal effects are likely even more important for cluster galaxy evolution than indicated by our H $\alpha$  study.

## 4. CONCLUSIONS

The results of our study of H $\alpha$  morphologies and cluster environmental effects in Virgo spirals include the following:

1. About half of Virgo spirals have truncated H $\alpha$  disks, which are relatively rare in isolated spirals (52% Virgo vs. 12% isolated). A small fraction of Virgo spirals are anemic (6% Virgo vs. 4% isolated), or truncated plus

anemic (8% Virgo vs. 0% isolated), or have enhanced star formation (8% Virgo vs. 0% isolated). 37% of the Virgo disks and 83% of the isolated spirals are classified as normal.

2. The cluster locations vary for the H $\alpha$  classes. Normal galaxies are virtually absent from the cluster core. Truncated galaxies are strongly concentrated in the core, but some are also found in the cluster outskirts. Anemic galaxies and those with enhanced NMSFRs are found throughout the cluster.

3. The widespread spatial truncation of H $\alpha$  disks and greater concentration of galaxies with truncated H $\alpha$  disks toward the cluster core provide evidence that ICM-ISM stripping is primarily responsible for the overall reduction of SFRs for Virgo spiral galaxies.

4. The fraction of anemic galaxies is modest in both environments, suggesting that starvation is not a major factor in the reduction of SFRs for Virgo spiral galaxies.

5. Several spirals have asymmetric H $\alpha$  enhancements at the outer edge of truncated H $\alpha$  disks, and at least two highly inclined spirals have extraplanar concentrations of HII regions, both suggestive of active ICM pressure. These galaxies are located as far as  $4.5^\circ \sim 1$  Mpc from M87. Their local star formation enhancements appear to cause only modest enhancements in the global star formation rates.

6. Three galaxies with luminosities of  $0.2-0.4L^*$  and one with  $2L^*$  have global and inner NMSFRs 2-3 times higher than any isolated sample galaxy. All are HI normal to HI rich, and are in apparent binary pairs and/or associated with large, extended clouds of HI, suggesting that tidal interactions and perhaps HI accretion within groups of galaxies falling into the cluster for the first time, are responsible for enhanced NMSFRs in an 8% minority of Virgo spirals.

7. There is a clear correlation, although not a perfect one-to-one correspondence, between the HI and H $\alpha$  radial distributions of large Virgo spirals. The galaxies with severely truncated HI disks also have the most truncated H $\alpha$  disks. The most anemic galaxies in H $\alpha$  are generally those with low HI surface densities across the disk. Galaxies with more peculiar HI morphologies also tend to have peculiar H $\alpha$  morphologies.

8. At least two classes of galaxies with severely truncated star-forming disks are identified. The most common type shows ‘simple truncation’, in which the inner disk star formation rates are similar to those in low  $C30$  isolated galaxies, but there is no star formation beyond  $0.3-0.4 r_{24}$ . This peculiar morphology has resulted in several cases in the assignment of a mixed Hubble type such as Sc/Sa, and in other cases an early spiral Hubble type. The morphology of these galaxies is most likely due to ICM-ISM interactions. The other type of severely truncated galaxies shows compact, non-axisymmetric, circumnuclear star formation. These properties are more likely due to gravitational interactions, including mergers.

9. These results support evidence that many of the lenticulars in  $z < 0.1$  rich clusters may indeed be stripped spirals, by demonstrating an intermediate population of small bulge spirals which are partially stripped, and misleadingly classified as Sa’s or other early types. Spirals which are stripped more severely and completely, as is likely in clusters with denser ICMs and higher velocity dispersions than in Virgo, would naturally be classified as lenticulars. In saying this we do not wish to imply that ICM-ISM stripping is the only mechanism driving lenticular formation in clusters. Some of the galaxies in Virgo with truncated H $\alpha$  disks are clearly much more peculiar than could be produced by ICM-ISM stripping, and have likely experienced tidal encounters or mergers. These peculiar systems are very HI-deficient and exhibit no detectable outer disk star formation, and have likely been stripped by the ICM in addition to experiencing a tidal encounter. In Virgo these are less common than the purely ISM-stripped spirals, but the ratio could well be different in other clusters.

We thank the referee Alessandro Boselli for his detailed comments which helped strengthen the paper. The funding for the research on the Virgo cluster and isolated spiral galaxies was provided by NSF grants AST-9322779 and AST-0071251. This research has made use of the NASA/IPAC Extragalactic Database (NED) which is operated by the Jet Propulsion Laboratory, California Institute of Technology, under contract with the National Aeronautics and Space Administration.

## REFERENCES

- Abadi, M. G., Moore, B., & Bower, R. G. 1999, MNRAS, 308, 947  
 Abraham, R. G., Smecker-Hane, T. A., Hutchings, J. B., Carlberg, R. G., Yee, H. K. C., Ellingson, E., Morris, S., Oke, J. B., & Rigler, M. 1996, ApJ, 471, 694  
 Balogh, M. L. & Morris, S. L. 2000, MNRAS, 318, 703  
 Balogh M. L., Morris, S. L., Yee, H. K. C., Carlberg, R. G., & Ellingson, E. 1999, 527, 54  
 Balogh, M. L., Navarro, J. F., & Morris, S. L. 2000, ApJ, 540, 113  
 Barnes, J. E. & Hernquist, L. 1991, ApJ, 370, L65  
 Bekki, K., Couch, W. J., & Shioya, Y. 2002, ApJ, 577, 651  
 Bertola, F., Corsini, E. M., Vega Beltran, J. C., Pizzella, A., Sarzi, M., Cappellari, M., & Funes, J. G. S. J. 1999, ApJ, 519, L127  
 Binggeli, B., Sandage, A., & Tammann, G. A. 1985, AJ, 90, 1681 (BST)  
 Binney, J., & Tremaine, S. 1987, Galactic Dynamics, (Princeton: Princeton University Press)  
 Böhringer, H., Briel, U.G., Schwarz, R.A., Voges, W., Hartner, G., Trümper, J. 1994, Nature, 368, 828  
 Boselli, A., Gavazzi, G., Donas, J., & Scodreggio, M. 2001, AJ, 121, 753  
 Bothun, G. D. & Sullivan, W. T. III 1980, ApJ, 242, 903  
 Bravo-Alfaro, H., Cayatte, V., van Gorkom, J. H., & Balkowski, C. 2000, AJ, 119, 580  
 Bravo-Alfaro, H., Cayatte, V., van Gorkom, J. H., & Balkowski, C. 2001, A&A, 379, 347  
 Byrd, G. & Valtonen, M. 1990, ApJ, 350, 89  
 Caldwell, N., Rose, J. A., Franx, M., & Leonardi, A. 1996, AJ, 111, 78  
 Caldwell, N., Rose, J. A., & Dendy, K. 1999, AJ, 117, 140  
 Cayatte, V., Kotanyi, C., Balkowski, C., & van Gorkom, J.H. 1994, AJ, 197, 1003  
 Couch, W. J., Barger, A. J., Smail, I., Ellis, R. S., & Sharples, R. M., 1998, ApJ 497, 188  
 Dale, D. A., Giovanelli, R., Haynes, M. P., Hardy, E., Campusano, L. E. 2001, ApJ, 549, 215  
 Davies, R. L. et al. 2001, ApJ, 548, 33  
 deVaucouleurs, G., deVaucouleurs, A., Corwin, H. G., Buta, R. J., Paturel, G., & Fouqué, P. 1991, Third Reference Catalog of Bright Galaxies (New York: Springer-Verlag)  
 Devereux, N. A. 1989, ApJ, 346, 126  
 Dressler, A. 1986, ApJ, 301, 35  
 Dressler, A. & Gunn, J. E. 1983, ApJ, 270, 7  
 Elmegreen, D. M., Elmegreen, B. G., Frogel, J. A., Eskridge, P. B., Pogge, R. W., Gallagher, A., & Iams, J. 2002, AJ, 124, 777  
 Gavazzi, G., Franzetti, P., Scodreggio, M., Boselli, A., Pierini, D. 2000, A&A, 361, 863  
 Gavazzi, G., Boselli, A., Mayer, L., Iglesias-Paramo, J., Vilchez, J.M. & Carrasco, L. 2001, ApJ, 563, L23  
 Giovanelli, R. & Haynes, M. P. 1983, AJ, 88, 881  
 Gunn, J. E. & Gott, J. R. 1972, ApJ, 176, 1  
 Haynes, M. P., Jore, K. P., Barlett, E. A., Broeils, A. H., & Murray, B. M. 2000, AJ, 120, 703

- Henriksen, M. J. & Byrd, G. 1996, *ApJ*, 459, 82
- Hensler, G., Tschöke, D., Bomans, D., & Boselli, A. 2003, *A&SS*, 284, 467
- Hernquist, L. 1992, *ApJ*, 400, 460
- Hernquist, L. 1993, *ApJ*, 409, 548
- Hernquist, L. & Quinn, P.J. 1988, *ApJ*, 331, 682
- Hibbard, J. E. 1995, PhD thesis, Columbia University
- Hoffman, G. L., Lu, N. Y., Salpeter, E. E., Farhat, B., Lamphier, C., & Roos, T. 1993, *AJ*, 106, 39
- Hoffman, G. L., Lu, N. Y., Salpeter, E. E., & Connell, B. M. 1999, *AJ*, 117, 811
- Hoffman, G. L., Salpeter, E. E., Farhat, B., Roos T., Williams, H. & Helou, G. 1996, *ApJS*, 105, 269
- Jones, L., Smail, I., & Couch, W.J. 2000, *ApJ*, 528, 118
- Kenney, J. D. P., Koopmann, R. A., Rubin, V.C., & Young, J. S. 1996, *AJ*, 111, 152
- Kenney, J. D. P. & Koopmann, R. A. 1999, 117, 181
- Kenney, J. D. P., Rubin, V. C., Planesas, P., & Young, J. S. 1995, *ApJ*, 438, 135
- Kenney, J.D.P., van Gorkom, J. H., & Vollmer, B. 2004, *AJ*, in press (June 2004) (astro-ph/0403103)
- Kenney, J.D.P., Young, J.S. Hasegawa, T., & Nakai, N. 1990, *ApJ*, 353, 460
- Kenney, J.D.P. & Yale, E. E. 2002, *ApJ*, 567, 865
- Kennicutt, R. C. 1989, *ApJ*, 344, 685
- Kennicutt, R. C. & Kent, S. M. 1983, *AJ*, 88, 1094
- Kennicutt, R. C., Roettiger, K. A., Keel, W. C., van der Hulst, J. M., & Hummel, E. 1987, *AJ*, 93, 1011
- Kennicutt RC, 1998, in *Galaxies: Interactions and Induced Star formation*, Saas-Fee Advanced Course 26, ed. D. Friedli, L. Martinet, D Pfenniger. (Berlin: Springer)
- Kewley, L. J., Heisler, C. A., Dopita, M. A., Lumsden, S. 2001, *ApJS*, 132, 37
- Koopmann, R.A. & Kenney, J.D.P. 1998, *ApJ*, 497, L75
- Koopmann, R. A., Kenney, J. D. P., Young, J. 2001, *ApJS*, 135, 125 (PI)
- Koopmann, R.A. & Kenney, J.D.P. 2003, submitted (PIII)
- Larson, R. B., Tinsley, B. M., & Caldwell, C. N. 1980, *ApJ*, 237, 692
- Lee, M. G., Kim, E., & Geisler, D. 1997, *AJ* 114, 1824
- Malin, D. 1993, *A View of the Universe* (Cambridge: Sky Publishing Corp.)
- Malin, D. 1994, in "Astronomy from Wide Field Imaging: Proceedings of IAU Symposium 161", ed. MacGillivray, H. T. et al. (Kluwer: Dordrecht), 567.
- Malkan, M. A., Gorjian, V., & Tam, R. 1998, *ApJS*, 177, 25
- Mamon, G. A., Sanchis, T., Salvador-Solé, E., & Solanes, J. M. 2004, *A&A*, 414, 445
- Mihos, J. C. 2004, in "Clusters of Galaxies: Probes of Cosmological Structure and Galaxy Evolution", ed. J. S. Mulchaey, A. Dressler, & A. Oemler (Cambridge: Cambridge Univ. Press), 278
- Miller, R. H. 1988, *Comm.Astrop.* 13, 1
- Moore, B., Lake, G., & Katz, N. 1998, *ApJ*, 495, 139
- Moss, C., & Whittle, M. 2000, *MNRAS*, 317, 667
- Nulsen, P. E. J. 1982, *MNRAS*, 198, 1007
- O'Connell, R. W. 1999, *Ap&SS*, 267, 329
- Oemler, A., Jr. 1992 in *Clusters and Superclusters of Galaxies*, ed. A.C. Fabian (Dordrecht: Kluwer), 29
- Phookun, B. & Mundy, L. G. 1995, *ApJ*, 453, 154
- Poggianti, B. M., Smail, I., Dressler, A., Couch, W. J., Barger, A. J., Butcher, H., Ellis, R. S., & Oemler, A., Jr. 1999, *ApJ*, 518, 576
- Poggianti, B.M. et al. 2001, *ApJ*, 563, 118
- Quilis, V., Moore, B., & Bower, R. 2000, *Science*, 288, 1617
- Richter, O.-G., Sackett, P. D., & Sparke, L. S. 1994, *AJ*, 107, 99
- Rix, H-W, Franx, M., Fisher, D., & Illingworth, G. 1992, *ApJ*, 400, 5
- Rose, J. A., Gaba, A. E., Caldwell, N., & Chaboyer, B. 2001, *AJ* 121, 793
- Rubin, V. C., Graham, J. A., & Kenney, J. D. P. 1992, *ApJ*, 394, 9
- Rubin, V.C., Waterman, A.H., & Kenney, J.D.P. 1999, *AJ*, 118, 236
- Sanchis, T., Lokas, E. L., & Mamon, G. A. 2004, *MNRAS*, 347, 1198
- Sandage, A., & Bedke, J. 1994, *The Carnegie Atlas of Galaxies* (Washington: Carnegie)
- Sandage, A., & Tammann, G. A. 1987, *A Revised Shapley-Ames Catalog of Bright Galaxies* (Washington: Carnegie)
- Schneider, S. E., & Corbelli, E. 1993, *ApJ*, 414, 500
- Schulz, S., & Struck, C. 2001, *MNRAS*, 328, 185
- Schweizer, F. & Seitzer, P. 1988, *ApJ*, 328, 88
- Solanes, J. M., Manrique, A., Garcia-Gomez, C., Gonzalez-Casado, G., Giovanelli, R., & Haynes, M. P. 2001, *ApJ*, 548, 97
- Struck, C. 1999, *Physics Reports*, 321, 1
- Toomre, A. & Toomre, J. 1972, *ApJ*, 178, 623
- Treu, T., Ellis, R. S.; Kneib, J.-P., Dressler, A., Smail, I., Czoske, O., Oemler, A., Natarajan, P., 2003, *ApJ*, 591, 53
- van den Bergh, S. 1976, *ApJ*, 206, 883
- van den Bergh, S., Pierce, M.J., & Tully, R. B. 1990, *ApJ*, 359, 4
- van Dokkum, P. G., Franx, M., Fabricant, D., Kelson, D. D., Illingworth, G. D. 1999, 520, 95
- van Driel, W. & van Woerden, H. 1989, *A&A*, 225, 317
- van Driel, W. & van Woerden, H. 1991, *A&A*, 243, 71
- van Gorkom, J. H., in "Clusters of Galaxies: Probes of Cosmological Structure and Galaxy Evolution", ed. J. S. Mulchaey, A. Dressler, & A. Oemler (Cambridge: Cambridge Univ. Press), 306
- Vollmer, B., 2003, *A&A*, 398, 525
- Vollmer, B., Cayatte, V., Balkowski, C., & Duschl, W. J. 2001, *ApJ*, 561, 708
- Vollmer, B., Beck, R., Kenney, J.D.P., & van Gorkom, J. H. 2004, *AJ*, in press (June 2004) (astro-ph/0403054)
- Vollmer, B., Marcelin, M., Amram, P., Balkowski, C., Cayatte, V., & Garrido, O. 2000, *A&A*, 364, 532
- Warmels, R. H. 1988, *A&AS*, 72, 19

TABLE 3  
H $\alpha$  PROPERTIES AND MORPHOLOGIES

(1) Name	(2) Star Formation Class	(3) RSA/BST	(4) RC3	(5) $M_B$	(6) $v_{he}$ (km s $^{-1}$ )	(7) $D_{87}$ ( $^{\circ}$ )	(8) HI Def	(9) CH $\alpha$	(10) EW tot ( $\text{\AA}$ )	(11) EW in ( $\text{\AA}$ )	(12) Comments on H $\alpha$ or Stellar Morphology
NGC 4064	T/C	SBc(s):	SB(s)a:pec	-18.72	913	8.8	1.23	0.97	8	19	
NGC 4178	N	SBc(s)II	SB(rs)dm	-19.13	378	4.7	-0.09	0.15	44	26	EEH
NGC 4189	N	SBc(sr)II.2	SAB(rs)cd?	-18.49	2115	4.3	0.27	0.15	27	14	EEH
NGC 4192	N	SbII:	SAB(s)ab	-20.10	-142	4.8	0.18	0.17	13	7	
NGC 4212	T/N	Sc(s)II-III	SAc:	-19.16	-81	4.0	0.16	0.37	18	17	
NGC 4237	T/N	Sc(r)II.8	SAB(rs)bc	-18.65	867	4.4	0.50	0.55	10	11	
NGC 4254	N	Sc(s)I.3	SA(s)c	-20.59	2407	3.6	-0.14	0.32	36	25	
NGC 4293	T/A	Sa pec	(R)SB(s)0/a	-19.82	893	6.4	1.45	1.00	1	4	tidally disturbed
NGC 4294	N	SBc(s)II-III	SB(s)cd	-18.40	355	2.5	-0.37	0.42	47	61	P (NGC 4299), EEH
NGC 4298	T/N	Sc(s)III	SA(rs)c	-18.94	1135	3.2	0.08	0.45	13	16	P (NGC 4302)
NGC 4299	T/E	Scd(s)III	SAB(s)dm:	-18.16	232	2.4	-0.22	0.46	84	117	P (NGC 4294)
NGC 4303	E	Sc(s)I.2	SAB(rs)bc	-20.85	1566	4.8	-0.03	0.49	61	62	
NGC 4321	T/N	Sc(s)I	SAB(s)bc	-20.91	1571	3.9	0.21	0.46	18	21	
NGC 4351	T/N(s)	Sc(s)II.3	SB(rs)ab:pec	-17.98	2310	1.7	0.37	0.77	16	32	off-center H $\alpha$
NGC 4380	T/A	Sab(s)II-III	SA(rs)b:	-18.66	967	2.7	0.66	0.77	4	5	EEH
NGC 4383	E	Amorph	Sa? pec	-18.34	1710	4.3	-0.53	0.84	73	89	
NGC 4394	A	SBb(sr)I-II	(R)SB(r)b	-19.26	922	5.9	0.39	0.25	5	3	
NGC 4405	T/N (s)	Sc(s)/S0	SA(rs)0/a:	-18.03	1747	4.0	0.85	0.91	10	19	EEH
NGC 4411B	N	Sc(s)II	SAB(s)cd	-18.10	1270	3.6	0.60	0.35	20	22	
NGC 4413	T/N	SBbc(rs)II-III	SB(rs)ab:	-18.05	102	1.1	0.26	0.58	16	25	
NGC 4419	T/A	Sa	SB(s)a	-18.89	-261	2.8	0.78	0.64	2	3	
NGC 4424	T/C	Sa pec	SB(s)a:	-18.70	439	3.1	0.79	1.00	10	24	merger
IC 3392	T/N (s)	Sc/Sa	SAB:	-17.72	1687	2.7	0.96	0.82	7	17	
NGC 4450	T/A	Sab pec	SA(s)Aab	-20.09	1954	4.7	0.99	0.69	2	3	
NGC 4457	T/N (s)	RSb(rs)II	(R)SAB(s)0/a	-19.26	882	8.8	0.92	0.66	8	12	one strong H $\alpha$ arm
NGC 4498	N	SBc(s)II	SAB(s)d	-18.40	1507	4.5	0.16	0.25	31	24	
NGC 4501	T/N	SBc(s)II	SAB(s)ab:	-20.75	2281	2.0	0.34	0.44	15	15	
NGC 4519	N	SBc(rs)II.2	SB(rs)d	-18.68	1220	3.8	-0.18	0.14	52	20	P (NGC 4519A)
NGC 4522	T/N (s)	Sc/Sb:	SB(s)cd:pec	-18.29	2328	3.3	0.69	0.56	17	34	extraplanar HII
NGC 4527	N	Sb(s)II	SAB(s)bc	-19.70	1736	9.8	-0.19	0.29	27	19	
NGC 4532	E	SmIII	IBm	-18.72	2012	6.0	-0.35	0.82	105	115	P (DDO137)
NGC 4535	N	SBc(s)I.3	SAB(s)c	-20.51	1961	4.3	0.16	0.17	28	17	
NGC 4536	N	Sc(s)I	SAB(rs)bc	-20.01	1804	10.2	0.17	0.46	23	28	
NGC 4548	A	SBb(rs)I-II	SB(rs)b	-20.04	486	2.4	0.76	0.11	4	1	
NGC 4561	N	SBcIV	SB(rs)dm	-18.06:	1407	7.0	-0.64	0.30	43	33	
NGC 4567	T/N	Sc(s)II-III	SA(rs)bc	-18.94	2274	1.8	0.64	0.55	16	20	P (NGC 4568)
NGC 4568	T/N	Sc(s)III	SA(rs)bc	-19.32	2255	1.8	0.64	0.62	23	32	P (NGC 4567)
NGC 4569	T/N (s)	Sab(s)I-II	SAB(rs)ab	-20.77	-235	1.7	0.92	0.92	4	9	extraplanar HII
NGC 4571	N	Sc(s)II-III	SA(rs)d	-19.21	342	2.4	0.49	0.27	13	10	
NGC 4579	T/N	Sab(s)II	SAB(rs)b	-20.46	1519	1.8	0.63	0.61	8	9	bl T/A
NGC 4580	T/N (s)	Sc/Sa	SAB(rs)a pec	-18.53	1034	7.2	1.31	0.93	5	11	
NGC 4606	T/C	Sa pec	SB(s)a:	-18.33	1664	2.5	1.16	0.53	4	8	P? (NGC 4607)
NGC 4639	N	SBb(r)II	SAB(rs)bc	-18.83	1010	3.1	0.18	0.25	19	10	
NGC 4647	N	Sc(rs)III	SAB(rs)c	-18.99	1422	3.2	0.43	0.44	24	27	P (NGC 4649), EEH
NGC 4651	N	Sc(r)I-II	SA(rs)c	-19.66	805	5.1	-0.28	0.56	22	21	minor merger
NGC 4654	N	SBc(rs)II	SAB(rs)cd	-19.88	1035	3.3	0.05	0.30	22	18	EEH
NGC 4689	T/N	Sc(s)II.3	SA(rs)bc	-19.47	1616	3.7	0.57	0.67	10	17	
NGC 4694	T/N	Amorph	SB0 pec	-18.83	1175	4.5	0.81	0.95	3	4	bl T/A
NGC 4698	A	Sa	SA(s)ab	-19.49	1002	5.8	-0.14	0.31	4	1	merger
NGC 4713	N	SBc(s)II-III	SAB(rs)d	-18.81	653	8.5	-0.35	0.28	59	45	
NGC 4772	T/N	...	SA(s)a	-19.13	1040	11.7	0.07	0.43	6	5	merger, bl T/A
NGC 4808	N	Sc(s)III	SA(s)cd:	-18.46:	766	10.2	-0.68	0.24	43	27	

NOTE. — (1) Name of galaxy, (2) Star Formation Class, where N=Normal, A=Anemic, E=Enhanced, T/A=Truncated/Anemic, T/C=Truncated/Compact, T/E=Truncated/Enhanced, T/N=Truncated/Normal, T/N(s)=Truncated/Normal (severe), (3) Hubble types from BST or Sandage & Tammann (1987) or Sandage & Bedke (1994), (4) Hubble type from deVaucouleurs et al. (1991), as provided by NASA/IPAC Extragalactic Database (NED), (5) the total, face-on absolute blue magnitude ( $M_B$ ), derived from deVaucouleurs et al. (1991), assuming a distance of 16 Mpc, (6) the heliocentric radial velocity, (7) the projected angular distance in degrees of the galaxy from M87, (8) the HI deficiency parameter, which was calculated as described in PIII, (9) the central H $\alpha$  concentration, (10) the H $\alpha$  equivalent width, calculated as in PIII, over the whole disk, (11) the H $\alpha$  equivalent width, calculated as in PIII, over the inner  $0.3r_{24}$  disk, (12) comments about galaxy characteristics, such as the presence of edge-enhanced H $\alpha$  emission (EEH), borderline T/A (bl T/A), membership in a pair (P(name of pair galaxy)), and/or evidence of a merger or tidal interaction. See text for references.

This figure "f4.jpg" is available in "jpg" format from:

<http://arXiv.org/ps/astro-ph/0406243v1>

This figure "f5.jpg" is available in "jpg" format from:

<http://arXiv.org/ps/astro-ph/0406243v1>

This figure "f6.jpg" is available in "jpg" format from:

<http://arXiv.org/ps/astro-ph/0406243v1>

This figure "f7.jpg" is available in "jpg" format from:

<http://arXiv.org/ps/astro-ph/0406243v1>

This figure "f8.jpg" is available in "jpg" format from:

<http://arXiv.org/ps/astro-ph/0406243v1>

This figure "f9.jpg" is available in "jpg" format from:

<http://arXiv.org/ps/astro-ph/0406243v1>

This figure "f10.jpg" is available in "jpg" format from:

<http://arXiv.org/ps/astro-ph/0406243v1>

This figure "f11.jpg" is available in "jpg" format from:

<http://arXiv.org/ps/astro-ph/0406243v1>

This figure "f12.jpg" is available in "jpg" format from:

<http://arXiv.org/ps/astro-ph/0406243v1>